Endoplasmic Reticulum contact sites facilitate the coordinated division of *Salmonella*-containing vacuole (SCV)

Umesh Chopra[1], Priyanka Bhansali[1], Subba Rao Gangi Setty[1], Dipshikha Chakravortty[1,2]

[1]Department of Microbiology and Cell Biology, Indian Institute of Science, Bangalore, Karnataka 560012, India

[2]School of Biology, Indian Institute of Science Education and Research Thiruvananthapuram, Maruthamala PO, Vithura, Thiruvananthapuram - 695551, Kerala, India

Corresponding author: Prof. Dipshikha Chakravortty

Email: dipa@iisc.ac.in

Abstract

Salmonella Typhimurium (STM) resides in a membrane-bound compartment called *Salmonella* Containing Vacuole (SCV) in several infected cell types. Within host cells, the division of bacteria and SCV are synchronous to maintain the single bacterium per vacuole. However, the mechanism regulating the synchronous fission and the machinery is not well understood. The fission of several intracellular organelles is regulated by the dynamic nature of the tubular endoplasmic reticulum (ER). In this study, we have evaluated the role of ER in controlling SCV fission. Interestingly, *Salmonella*-infected cells show the activation of unfolded protein response (UPR) with expanded ER tubules compared to the uninfected cells. Further, changing the ratio/expression of ER morphology regulators, such as reticulon-4a (Rtn4a) and CLIMP63, affected bacterial proliferation significantly, suggesting a potential role for tubular ER in facilitating the SCV division. Live-cell

imaging analysis shows the marking of tubular ER precisely at the center of the majority of SCV division (78%) sites. We have investigated the role of SteA, a known *Salmonella* effector, in modulating the membrane dynamics and coordinating the SCV division. We observed that SteA resides on the SCV membranes and helps in making membrane contact sites between SCV and ER. Accordingly, the colocalization of ER with SCV enclosing steA mutant *Salmonella* was significantly reduced compared to SCV-formed by wild-type *Salmonella*. Depletion of *steA* in *Salmonella* resulted in profound defects in SCV division, resulting in multiple bacteria residing in a single vacuole with defects in proliferation compared to the wild-type strain in epithelial cells. However, during infection in mice, the STM*ΔsteA* mutant did not show any defect in colonization but affected the survival rate of mice. Overall, this study suggests a coordinated role of bacterial effectors in promoting the ER contact sites with SCVs and thus regulating the successful division of pathogenic vacuole.

36 **Introduction**

37 *Salmonella enterica* subsp. *enterica* serovar Typhimurium (STM) is an intracellular pathogen
38 known to infect a wide range of hosts and result in diseases across species, including gastroenteritis
39 to systemic infections[1,2]. *S.* Typhimurium enters the body through the fecal-oral route following
40 the bacteria utilize an arsenal of strategies to overcome several stresses like the acidic pH of the
41 stomach, gut flora, bile salts, etc., and finally reach the small intestinal epithelia[3]. *Salmonella*
42 secretes several virulence proteins inside the cell which lead to actin rearrangement and membrane
43 ruffling, that helps in the invasion of bacteria inside the host epithelial cell[4–7]. *Salmonella* effector
44 sopD is known to facilitate the recruitment of dynamin2 (Dyn2) at the invasion site, which helps
45 in the endocytosis of bacteria inside host cells[8].

46 Upon invasion into the host cell, *Salmonella* resides in *Salmonella* containing Vacuole (SCV), a
47 membrane-enclosed compartment. Mature SCV shares several characteristics markers of
48 lysosomes/late endosomes such as LAMP1 and Rab7 but is negative for acid hydrolases and
49 cathepsins[9]. Inside the epithelial cells, several protruding structures from SCV known as
50 *Salmonella*-induced filaments (SIFs)[10,11] are observed which as LAMP1 positive. The membrane
51 composition of SCV is not very well understood but it contains molecules and proteins from
52 several host organelles and are enriched with several bacterial effector proteins[12,13]. Our group as
53 well as several others have previously shown that *Salmonella* resides as a single bacterium per
54 vacuole state inside the host, suggesting that SCV membrane divides synchronously with the
55 division of *Salmonella* but the mechanism behind SCV division is not known[14–17]. For successful
56 SCV division, expansion of SCV membrane, pinching of SCV membrane precisely with bacterial

division, and lastly, scission of host-derived SCV membrane must be followed in an orchestrated manner.

Several literatures have highlighted the importance of contact sites between several organelles such as ER with mitochondria, plasma membrane and endosomes, and mitochondria with lysosomes[18–21]. Contact sites between ER-mitochondria and ER endosomes are very widely studied in the aspect of organelle division[18,22]. In the case of mitochondria that comprises of an inner and an outer membrane, and both membranes divide simultaneously during its fission. The inner mitochondrial membrane uses its machinery for fission while outer membrane constriction is initiated by the ER followed by the recruitment of Drp1, which mediates the fission of mitochondria[18,23,24]. Bacterial pathogens like *Chlamydia* and *Brucella* make contact sites with cellular organelles to facilitate their proliferation inside the host cell[25–27]. Interestingly, the SCV membrane also comprises of several ER proteins, and recently membrane contact sites between SCV and ER have also been observed [28]. To understand the mechanism behind the SCV division, we reasoned that SCV is partially like mitochondria as far as the origin of the membrane is concerned. SCV and mitochondria (being an endosymbiont) encompass an outer membrane derived from the eukaryotic host while the inner membrane of mitochondria is prokaryotic in nature like the cell wall of *Salmonella*. To understand the same, we hypothesized that a process similar to mitochondria could lead to SCV fission. Our results suggest that *Salmonella* infection leads to activation of UPR, ER expansion, and an increase in tubulation. We have observed ER tubules mark at the fission site of SCV division which possibly initiate the constriction. *Salmonella* translocated effector steA localizes onto the SCV membrane and possibly helps in making contact with ER, suggesting that steA can act as a factor to recruit the ER onto SCV and thus facilitate the SCV division. STM*ΔsteA* resides as multiple bacteria in one big vacuole with defects in

80 proliferation. In the mice model, STM*ΔsteA* doesn't show any defect in colonization in the
81 secondary site of infection, however, there is a delay in the onset of mice death upon infection as
82 compared to STM WT. Overall, our study unravels for the first time, the coordinated role of ER
83 and bacterial effector steA in bacterial proliferation inside the cell.

84

85

86 **Materials and Methods**

87 **Bacterial strains and culture conditions**

88 *Salmonella enterica* subspecies *enterica* serovar Typhimurium (STM WT) wild-type strain ATCC
89 14028s was used in all experiments. The bacterial strain was cultured in Luria broth (LB-Himedia)
90 with constant shaking (170 rpm) at 37°C orbital-shaker. Antibiotics like kanamycin (50 µg/ml),
91 and ampicillin (50µg/ml) were used wherever required. A one-step gene inactivation method was
92 used for the generation of knockout strains[29]. Wild type as well mutant strains were transformed
93 with pFPV-m-cherry or pFPV-GFP plasmid for immunofluorescence assays.

94 Table:1 List of bacterial strains used in this study

Strain	Characteristic (Antibiotic resistance)	Source
STM WT 14028s	-	Kind gift by Prof. M. Hensel
STM*ΔssaV*	Kan^R	Laboratory stock
STM*ΔsteA*	Kan^R	This study
STM*ΔsteA:steA*	Kan^R +Amp^R	This study

95

96 **Generation of Complement strain and steA-eGFP plasmid**

97 Low copy number plasmid pQE-60 was used to prepare the steA-HA complement strain. Briefly,
98 PCR amplification (using Thermo Q5 DNA polymerase) of the *steA* gene was performed using
99 Wild Type STM colony with respective PCR primers. Forward cloning primer was chosen from a
100 position of 250 base pairs upstream of the gene start site, to amplify the native promoter of the
101 gene during PCR and to maintain native expression level of protein and sequence of HA tag was
102 added in reverse primer. The amplified PCR product was purified using a Gel extraction kit
103 (Qiagen). The PCR product and Plasmid were subjected to restriction digestion by using Xho1
104 (NEB) and Hind III (NEB) at 37°C for 2 hours. Double digested PCR product and plasmid were
105 further subjected to Ligation using T4 DNA ligase (NEB) at 16°C for 12-14 hours. The ligated
106 product was further electroporated in STMΔ*steA* strain to prepare the complemented strain i.e.
107 STM*ΔsteA*:pQE60-*steA* (hence referred to as STM*ΔsteA:steA*). The expression level of
108 complement was confirmed with western blotting and confirmed with DNA sequencing.

109 For preparation of steA-eGFP plasmid for transfection study, eGFP-N3 empty vector was used.
110 The sequence of steA was amplified via PCR from STM WT using primer with restriction site for
111 Xho1 and BamH1. The entire process for cloning was performed as discussed above.

112 **Eukaryotic Cell Culture, Transfection and Plasmids**

113 HeLa cells and RAW 264.7 murine macrophages were cultured in DMEM (Lonza) containing 10%
114 FBS (Gibco) at a humified incubator maintaining a temperature of 37°C and 5% CO_2. Cells were

115 seeded in 6 wells, 12 wells, or 24 well plates at a confluency of 60-70% prior to infection. Cells
116 were maintained in the presence of 1% penstrep. Cells were given a PBS wash and supplemented
117 with fresh media without penstrep at least 6 hours prior to infection. Plasmid overexpression or
118 knockdown via shRNA was done using Lipofectamine 3000 using manufacturer protocol. Briefly,
119 300ng of plasmid was mixed in opti-MEM media for 5 min while 1ul of L3000 was mixed (for
120 one well of 24 well plate) in opti-MEM for 5 min separately and further mixed and incubated for
121 20 min at room temperature. Post incubation, this mixture was added to cells for 6 hours, for
122 transfection to take place. Cells were washed with PBS and supplemented with complete media
123 post 6 hours of treatment, and post 48h of transfection, infection was given. Overexpression
124 constructs such as: pHAGE2 mCherry-Rtn4a was a kind gift from Prof. Tom Rapoport (Addgene
125 plasmid 86683)[30] mCh Climp-63 and mCh sec61β was a kind gift from Prof. Gia Voeltz (Addgene
126 plasmid 136293, Addgene 49155)[31,32], RFP KDEL construct was a kind gift from Prof. Nagaraj
127 Balasubramanian[33], GFP-LAMP1 was provided by Prof. Mahak Sharma[34]. The shRNA plasmids
128 were obtained from the human genome-wide TRC shRNA library (purchased from Sigma-Aldrich,
129 USA, Catalog no. SH0411), available at shRNA resource centre, MCB, IISc. pLKO.1-puro non-
130 mammalian shRNA (SHC002, shControl) was used as a control in all the shRNA mediated
131 knockdown experiments. Plasmid sequences and details are added in supplementary table 3.

132 **Protocol for infection (Gentamicin Protection Assay)**

133 The cells were seeded at the required confluency and infected with *Salmonella* strains with actively
134 growing log phase culture (for epithelial cells) and stationary phase culture (for RAW 264.7
135 macrophages) at Multiplicity of infection (MOI) 10 for Intra Cellular Survival Assay (ICSA) and
136 confocal imaging. For the live cell imaging experiment, an MOI of 25 was used to increase the

137 event of finding infected cells for imaging. For confocal microscopy studies, cells were seeded on
138 sterile glass coverslips at least 24 hours before infection. Upon infecting the cells at the required
139 MOI, the plate was centrifuged at 600 rpm for 5 min to facilitate the adhesion, and then the plate
140 was incubated for 25 min at 37°C and 5% CO_2. Post incubation, bacteria-containing media was
141 removed, and cells were given 2 PBS washes to remove any extracellular bacteria. Fresh media
142 containing 100µg/ml of gentamicin was added into wells and incubated at 37°C for one hour.
143 Following this, cells were again given 2 PBS washes, and fresh media containing 25µg/ml of
144 gentamicin was added and this concentration was maintained till the end point of the experiment.
145 Cells were harvested at required time points such as 2h and 16h for ICSA, 2h, 6h, and 16h for
146 confocal microscopy-based experiments.

147 **Confocal Microscopy**

148 After an appropriate hour post-infection, cells were washed with PBS twice and fixed with 3.5%
149 PFA at room temperature for 15 min. After fixation, coverslips were washed with PBS, and cells
150 were stained with primary antibody prepared in 2% BSA in PBS carrying 0.01% of saponin (for
151 membrane permeabilization) for 1 hour at room temperature or 4°C overnight in a cold room as
152 required. Post incubation, coverslips were washed again twice with PBS and incubated with
153 specific secondary fluorophore-labeled antibodies and incubated for one hour at room temperature.
154 Coverslips were then mounted on clean glass coverslips using mounting media. Once the mounting
155 media was dried, coverslips were stabilized by sealing the periphery with transparent nail paint on
156 the sides. Images were acquired on a confocal scanning laser microscope (Zeiss 880 multiphoton
157 microscope or Leica sp8 falcon system with or without zoom as required). Zen black software was
158 used for all colocalization-based quantification and to calculate mean fluorescence intensity (MFI).
159 Calculations of CTCF, percent of ER tubules, SCV diameter, and Line scans were prepared using

160 ImageJ. Live cell microscopy was performed on Leica SP8 Falcon microscope and live cell video
161 was processed and prepared using LAS X software. Antibodies used in this study is mentioned in
162 supplementary table 2.

163 **Bacterial enumeration after infection for Intracellular survival assay**

164 After the appropriate hour of post-infection, cells were washed with PBS at RT and lysed using
165 0.1% Triton-X 100. Cell lysate was plated on SS agar to obtain colony forming unit (CFU) and it
166 was used for the calculation of Percent Invasion and Fold proliferation using this formula.

167 Percent Invasion: (CFU obtained at 2 hours post infection/ CFU obtained from pre-inoculum) *100

168 Fold proliferation: CFU obtained at 16-hour post-infection/CFU obtained at 2 hours PI

169 **RNA isolation and Real-Time PCR (qRT-PCR)**

170 RNA isolation was performed using TRIzol (Takara) following the manufacturer's protocol.
171 Quantification of RNA was done using nano-drop (Thermo-Fisher Scientific) and RNA samples
172 were run on 1% agarose gel to check the quality of RNA. 2 µg of RNA was subjected to DNase I
173 (Thermo Fischer Scientific) treatment at 37°C for 1 hr followed by addition of 0.5M EDTA (final
174 concentration 5mM) and heat inactivation at 65°C for 10 mins to inactivate the enzyme. Further
175 cDNA was prepared by using a cDNA synthesis kit (Takara) as per the manufacturer's instructions.
176 The expression profile of all genes of interest was evaluated using RT primers by using SYBR
177 green mix (Takara) in a Biorad Real-Time PCR machine. The expression value of the target gene
178 was normalized to housekeeping internal control β-actin and further compared with uninfected
179 cells. Primers used in this study are mentioned in supplementary Table 1.

180 ***In vivo* animal experiment**

181 6-8 weeks old C57BL/6 female mice were infected by orally gavaging 10^7 CFU of STM WT,

182 STM*ΔsteA* and STM*ΔsteA:steA*. 5 days post-infection, mice were euthanized and organs such as
183 liver, spleen, MLN, and blood were harvested to study the colonization in organs. To enumerate
184 CFU,
185 organs were homogenized and further plated on *Salmonella-Shigella* agar. Obtained CFU values
186 were normalized with the gram weight of the organ and then converted into a log scale. Blood
187 was collected through heart puncture and plated on SS agar. For the mice survival assay, 10^8
188 CFU was administered to each mouse via oral gavage. Mice were monitored every day till the
189 time none of the mice in the cohort survived. The animal experiments were carried out in
190 accordance with the approved guidelines of the institutional animal ethics committee at the
191 Indian Institute of Science, Bangalore, India (Registration No: 48/GO/ReRcBiBt-S/Re-
192 L/99/CPCSEA). All procedures involving the use of animals were performed according to the
193 Institutional Animal Ethics Committee (IAEC)-approved protocol, ethics number:
194 CAF/Ethics/853/2021.
195
196 **Statistical analysis:**
197 Statistical analysis was performed using GraphPad prism software. For analysis, the student's t-
198 test (unpaired parametric test) was performed. The results are indicative of mean± SD or mean±
199 SEM. For animal experiments, the Mann-Whitney test was performed. Group size, experimental
200 number, no of cells in each set, and P value of each experiment are described in figure legends.
201
202
203
204

205

206

207 **Results**

208 ***Salmonella* infection leads to the activation of UPR and expansion of the Endoplasmic**
209 **Reticulum**

210 Several bacterial and viral infections are known to activate UPR for their survival[35,36]. UPR helps
211 to alleviate the ER stress by initiating several transcriptional and translational regulations which
212 lead to the maintenance of ER homeostasis[37,38]. Inside the cell, UPR signaling is maintained by
213 transmembrane proteins located in the ER membrane and their catalytic domain towards the
214 cytosol. Inositol requiring enzyme-1 (IRE-1), Protein kinase c like ER kinase (PERK), and
215 Activating transcription factor-6 (ATF-6) comprises the main arm of UPR. Recent reports have
216 shown the contact of SCV with ER, also the presence of ER proteins in the membrane fraction of
217 SCV suggests the crosstalk between the two[28,12]. Here, we investigated how *Salmonella* infection
218 modulates the ER dynamics. To understand the activation of UPR by any of these pathways, we
219 used confocal microscopy to look at the downstream transcription factors such as XBP1, ATF4,
220 and ATF6 respectively inside the nucleus upon infection. SPI2 mutants of *Salmonella*, STM*ΔssaV*
221 (which is unable to secret SPI-2 encoded effector protein in host cytosol) was kept as a control to
222 understand if activation of UPR is mediated by bacterial effectors or dependent on bacterial
223 invasion. Our results suggest that from as early as post 2h of *Salmonella* infection, both the
224 transcription factors, ATF4 and ATF6 in the cytosol translocated to the nucleus of infected cells as
225 compared to uninfected cells, and STM*ΔssaV* infected cells, suggesting that only wild type

226 *Salmonella* can activate UPR (fig 1A-1D). *Salmonella* induced ATF4 and ATF6 signaling was
227 retained till 16h post-infection (fig S1A-S1D). However, we didn't observe XBP1 recruitment
228 inside the nucleus (fig 1E,1F) upon infection at any time point post-infection (fig S1E, S1F)
229 suggesting that *Salmonella* infection upregulates UPR by PERK and ATF6 pathways. To alleviate
230 the ER stress, activation of UPR leads to the expansion of the ER, protein folding capacity, and
231 increased phospholipid production[40]. Increased bacterial proliferation requires a continuous source
232 of membrane for the increasing number of SCV and increased phospholipid production upon UPR
233 could facilitate the SCV proliferation inside the host cell. Therefore, we sought to determine if
234 *Salmonella* infection led to ER expansion during the pathogenesis phase. Our transcriptional
235 analysis suggests that upon infection, there is upregulation at the transcript level of ER shaping
236 proteins such as Climp63 (responsible for maintaining ER sheets) and Reticulon-4a (Rtn4a,
237 essential for maintaining ER tubules) (fig 1G, fig 1H). The upregulation was significantly observed
238 at the late time point of infection, i.e., 16h post-infection, suggesting that active proliferation of
239 *Salmonella* and not just invasion (as evident at 2h and 6h post-infection) leads to ER expansion.

240 Since an increase in the transcript levels of ER shaping proteins were observed at the later time of
241 infection, we tried to quantify the percentage of ER sheets and tubules using ER marker, RFP-
242 KDEL upon infection as a measure to understand ER expansion upon infection. Upon analysis of
243 microscopy images, we observed that *Salmonella*-infected cells showed an increased percentage
244 of ER tubules compared to uninfected cells (fig1I, fig1J). The changes in percent ER tubules were
245 only evident in infected cells as compared to un-infected and bystander cells (neighboring cells
246 which are not infected), suggesting that stabilized SCV and bacterial effectors are responsible for
247 this phenotype (fig S1G and S1H). Together, this data indicates that *Salmonella* infection leads to
248 changes in ER morphology.

249 **Expansion of ER tubules facilitates SCV proliferation and its division**

250 Dynamic ER tubules play an essential role in forming membrane contact sites with several
251 organelles [41,42]. Fig1 indicates that actively proliferating bacteria increased tubular ER and
252 upregulated the expression of Rtn4a. We also tried to understand if there is an advantage of the
253 increased tubules to bacterial proliferation. To identify the role of ER tubules in mediating bacterial
254 proliferation, we transiently overexpressed reticulon 4a (Rtn4a) in HeLa cells, which helps to
255 increase ER tubules[43], and then quantified the proliferation of bacteria by intracellular survival
256 assay (ICSA). As compared to empty vector and general ER marker sec61β-mCh control,
257 increased ER tubulation by Rtn4a led to the higher proliferation of *Salmonella* with no significant
258 change in percent invasion, suggesting an increase in ER tubules helps in bacterial proliferation
259 (fig2A, figS2A). To validate if this change in proliferation was dependent solely on the function
260 of Rtn4a, knockdown of Rtn4a via shRNA was performed (figS2B). Knockdown of Rtn4a led to
261 reduced proliferation of bacteria as compared to scrambled control hence strengthening the crucial
262 role of ER tubules in bacterial proliferation (fig2B). Climp63 overexpression led to an increase in
263 ER sheets as opposed to tubules. We quantified the number of SCV per cell upon transiently
264 overexpressing the Climp63 in HeLa cells. Our data indicated that the number of SCV present per
265 cell decreases upon overexpressing ER sheets using Climp63 compared to controls (fig2C, fig2D).
266 Division of *Salmonella* is linked with the fission of SCV membrane [44]. Since the intricate balance
267 of ER sheets and tubules affects bacterial proliferation, we hypothesized that ER tubules might
268 facilitate SCV fission. In the case of mitochondria, membrane-less organelle, and endosomes, ER
269 marks the division site, and later fission is completed by Drp1 (in mitochondria) and coronin1c
270 and TMCC 1 complex (in endosome)[18,45–47]. To investigate this, we performed live cell imaging in
271 cells transfected by RFP-KDEL (to mark the ER) followed by infection with *Salmonella*.

272 Quantification of data suggests that ER tubules mark the division site precisely at the center of
273 dividing SCV in 78% of events (fig2E-G). STM WT infected RAW macrophage also showed
274 contact of ER on the dividing bacteria (S2C).This was also evident in fixed cell images where we
275 could observe Lamp1 enclosed bacterial division in SCV marked by ER tubules exactly in the
276 center in 56.7±6.61% of fission events, however, in 14±9.07% of events, ER was seen in proximity
277 to the center and hence named adjacent while 29.2±8.4% of dividing SCV did not possess ER
278 tubules on them (fig2H, fig2I). In the majority of STM WT-infected cells, SCV was observed near
279 the periphery of the cell, suggesting mature SCV migrates towards the cell periphery to make
280 contacts with ER tubules to facilitate its division (S2D).This data suggests the importance of ER
281 tubules in marking the fission site of SCV. Taken together this data suggests that ER tubules help
282 in the proliferation and division of SCV inside the cell and help in maintaining SCV number within
283 the cell.

284

285 ***Salmonella* translocated effector steA is crucial for maintaining SCV contact site with ER**
286 **resulting in a single bacterium per vacuole**

287 SCV division leads to a single bacterium per vacuole throughout the course of pathogenesis in cell
288 lines or in mouse liver model[14]. Domingues et al suggested the role of steA in maintaining the
289 membrane dynamics of SCV[48]. In accordance with the same, we also observed that steA mutant
290 strain of *Salmonella* (STM*ΔsteA*) resides as multiple bacteria in one single vacuole (fig 3A). Our
291 data suggests that compared to STM WT, 30±3% of mutant bacteria reside in one big vacuole,
292 suggesting that loss of function of steA leads to improper SCV fission (fig 3B). Live cell imaging
293 shows several points of contacts between SCV and ER, suggesting that SCV actively makes

294 membrane contact sites with ER for its survival and proliferation (fig2E, fig3C). SteA resides onto
295 the PI4P enriched SCV membrane (fig3C), and hence we asked are membrane contacts between
296 ER and SCV maintained by steA? Microscopy images show that steA-enriched SCV makes
297 contact with ER (fig3C). Quantification of the data suggests that ER colocalizes more with the
298 SCV of STM WT than the SCV formed by STM*ΔsteA*, suggesting that steA helps in making
299 contact sites of SCV with ER (fig3D, fig3E). This was also observed upon transfecting HeLa cells
300 with steA-eGFP construct. SteA-eGFP showed higher colocalization with ER marker RFP-KDEL
301 as compared to eGFP empty vector control, strengthening the fact that steA possibly associate with
302 ER (figS3A,S3B). This data suggests that steA might help in making contact sites with ER and
303 further recruiting ER onto the SCV. These contact sites can be used as a stealthy approach by
304 *Salmonella* to recruit membrane from ER, and along with other *Salmonella* effector proteins,
305 facilitating SCV fission.

306 **STM*ΔsteA* shows defect in proliferation inside epithelial cells and pathogenicity in mice in**
307 **vivo model**

308 Previous reports from our lab suggested that *Salmonella* utilizes the strategy of SCV division to
309 increase the number of SCV per cell, so it becomes difficult for the cellular system to eradicate the
310 growing SCV[14]. Since steA mutants form a big vacuole inside the cell, we asked how the mutant
311 strain proliferates in the cell. As compared to STM WT and steA complemented strain, STM*ΔsteA*
312 proliferated significantly less in the HeLa cell line while there was no difference in invasion rate
313 of bacteria inside cell (fig4A, figS4A). Less proliferation of mutant strain suggests that those bulky
314 vacuoles might be targeted by cellular machinery for degradation. Quantification of vacuole size
315 suggests that the diameter of SCV formed by STM*ΔsteA* is around 6.9±3.13µm whereas SCV of

316 STM WT is 0.4±0.11µm (fig4B, fig4C). Using LC3B as a marker to detect the extent of autophagy,
317 we observed that LC3B colocalized more with SCV of steA mutants as compared to SCV of STM
318 WT at 16h post-infection (fig4D,fig4E). Actively proliferating *Salmonella* also reduces the
319 number of lysosomes inside the cell to escape its fusion with acidic lysosomes[14.] In STM*ΔsteA*
320 infected cells, we observed a higher intensity of Lamp1 similar to uninfected cells, suggesting that
321 STM*ΔsteA* is unable to change the lysosomal dynamics as opposed to STM WT. Higher flux of
322 lysosomal proteins along with the recruitment of LC3B led to less proliferation of the STM*ΔsteA*
323 inside the cell (figS4B, figS4C). Next, we were interested in understanding the pathogenicity of
324 STM*ΔsteA* in an in vivo model. We orally gavaged C57BL/6 mice with 10^7 CFU of STM WT,
325 STM*ΔsteA*, and STM*ΔsteA:steA,* and 5 days post-infection, mice were euthanized, and organs such
326 as liver, spleen, and mesenteric lymph nodes were harvested since they act as a secondary site of
327 infection (fig4F-4I). We observed no significant change in the colonization of bacteria in these
328 organs, suggesting STM*ΔsteA* doesn't lose its capability to cross the gut barrier and colonizing and
329 dissemination in distal organs and blood (figS4D). However, upon performing a survival assay of
330 mice, we noticed the delayed onset of mice death in the STM*ΔsteA* infected cohort (fig4J), where
331 STM WT infected mice started succumbing to infection at 5th day post infection, STM*ΔsteA*
332 infected cohort started succumbing to infection at 7th day post infection. Taken together, this data
333 suggests that if the fission of SCV is altered, *Salmonella* resides as multiple bacteria in one big
334 vacuole and proliferates less. Those big/bulky vacuoles are further targeted by autophagic
335 machinery and cleared by active lysosomes in the cell culture system. However, in an in-vivo mice
336 model, colonization of bacterium is not hampered, but it affects the survival rate of mice,
337 suggesting that SteA acts as an essential effector for pathogenicity in mice.

338

339 **Discussion:**

340 Bacterial pathogens invade several cell types and reside in endocytic or phagocytic vacuoles[49].
341 Cell uses their extraordinary machinery to clear the pathogens, but by using several effector
342 proteins, bacterial pathogens modulate cellular machinery and prolong their survival. A few
343 strategies that several bacterial pathogens utilize are: modification of the membrane of the
344 pathogen-containing vacuole, blocking the activation of xenophagy, and escaping its fusion with
345 acidic lysosome[50–56]. Bacterial pathogens such as *Legionella, Brucella, Chlamydia*, and
346 *Salmonella* are known to reside in vacuoles, but the morphology and membrane source of the
347 vacuole are quite different. *Legionella* and *Chlamydia* reside in a spacious vacuole that comprises
348 multiple bacteria in a single vacuole[57], contrary *Salmonella* resides in a tight-fitting vacuole as a
349 single bacterium per vacuole[14]. The biogenesis of the SCV membrane is not very well known but
350 proteome analysis of SCV suggests that the SCV membrane is highly modified and contain
351 proteins from the lysosome, Golgi, and ER[12]. Several effectors of *Salmonella* help in recruiting
352 membrane components, inhibiting the transport of M6PR, and making contact sites with organelles
353 for its proliferation [58–60]. Our results suggest that *Salmonella* infection induces ER stress inside the
354 cell and activates the UPR. A few ways by which UPR helps in alleviating stress are 1) by
355 increasing the protein folding capacity of cells and 2) by expanding the ER. Our data suggests that
356 wild-type STM infection leads to UPR activation while STM*ΔssaV* is unable to activate the UPR
357 arm. This suggests that bacterial effectors are crucial for initiating ER stress, as it was evident as
358 early as 2h post-infection. Our studies support the previous findings, which suggest *Salmonella*-
359 induced ER stress is crucial for bacterial proliferation[61–63]. Further, UPR activation leads to an
360 increase in phospholipid production[40], which could be useful for the bacteria as growing SCV
361 requires a continuous source of membrane. *Salmonella*-infected cells show an increase in

362 expression of *Reticulon-4a* and *Climp63* with an increase in tubular ER, suggesting this is an active
363 strategy employed by bacteria for its survival. Exogenously overexpression of Rtn4a provides an
364 advantage in the proliferation of *Salmonella* however, reduction in ER tubules by knockdown of
365 Rtn4a or overexpression of ER sheets using Climp63 adversely affects the bacterial proliferation
366 and SCV number inside the cell, indicating ER tubules plays a crucial role in bacterial
367 proliferation. The intricate balance of ER sheets and tubules has been recently shown to affect the
368 dynamics of membrane-less organelle[42]. Our study also highlights the importance of ER in the
369 successful proliferation of *Salmonella*. Our live cell data showed the recruitment of ER tubules at
370 the center of dividing SCV. This was evident in HeLa as well as RAW macrophage cell lines,
371 suggesting that ER tubule recruitment marks the division site of SCV. ER is very well known for
372 marking the division site of organelles such as mitochondria, membrane-less organelle, and
373 endosomes[18,42,64]. Our study suggests that *Salmonella* hijacks the strategy of ER recruitment for
374 its survival and SCV division. We have identified the role of bacterial effector SteA in maintaining
375 the contact of SCV with ER in the formation of possible membrane contact sites. Earlier studies
376 have shown the presence of steA on SCV and its colocalization with Golgi [65–67]. In our study, we
377 have partially observed a similar phenotype and have observed a new role of steA in interaction
378 with ER. Inside the infected cell, the expression of steA is highly regulated as it can be mostly seen
379 around the bacteria onto SCV. To investigate the role of steA in making contact sites, we looked
380 for the colocalization of ER with SCV of STM WT and STM*ΔsteA* and observed the difference in
381 colocalization of ER with SCV, highlighting the importance of *Salmonella* effector steA in
382 mediating contact site between SCV and ER. Bacterial pathogens such as *Chlamydia* use its
383 effector protein for forming contacts of its inclusion bodies with ER [25] and also it targets host
384 cellular protein to facilitate this interaction [68]. *Salmonella* effectors sseJ and sseL have previously

been reported to recruit OSBP1 onto SCV which helps in making contact with VapA and VapB (conserved ER proteins known for tethering of ER with cellular organelles) and maintain SCV vacuolar integrity [69]. Our data suggests the potential role of steA in forming contact sites of SCV with ER as a strategy to facilitate its proliferation.

The loss of function of steA led to a bulky vacuole carrying multiple bacteria inside and with defects in proliferation. Evidence from McQuate et al., also suggests the defect in the proliferation of STM*ΔsteA* in epithelial as well as macrophages [66]. To understand the difference in proliferation of STM*ΔsteA* compared to STM WT, we have observed SCV formed by STM*ΔsteA* colocalizes more with autophagy marker LC3B, suggesting big bulky vacuoles are cleared by the cellular system and hence lead to less proliferation inside the cell. STM WT also actively reduces lysosome number inside the cell as an active strategy to block its fusion with the acidic lysosome [14]. But in the case of STM*ΔsteA* infected cell, we observed a higher mean intensity of LAMP1 which was similar to intensity observed in uninfected cells suggesting that somehow STM*ΔsteA* could not modulate lysosomal dynamics and as a result, active lysosome could hinder the bacterial proliferation in cell line model. Similarly, Liu et al.,2021 have highlighted the importance of steA in bacterial proliferation inside cells by impairing the fusion of SCV with lysosomes[70]. Taken together this data suggests the importance of steA in bacterial proliferation inside infected cell. However, to our surprise, we did not observe any defect in the in vivo colonization of mouse organs such as the liver, spleen, MLN, and blood. Survival analysis of mice suggests late onset of mice death in STM*ΔsteA* infected cohort upon infection as compared to STM WT. We have also observed less weight reduction in STM*ΔsteA* infected mice as compared to STM WT and STM*ΔsteA:steA*, and this difference in weight reduction could benefit mice survival (figS4E). However, Geddes et al, 2005 have reported the importance of steA for efficient colonization in

408 mouse spleen using the Balb/c mice model infecting via the intraperitoneal route [65]. The difference
409 in colonization from our study can be dependent on the route of infection wherein, our study uses
410 a conventional way of oral gavaging for *Salmonella* infection which is a natural route of infection
411 in contrast to intraperitoneal injection. Taken together, our study suggests the importance of steA
412 in bacterial pathogenicity and proliferation.

413 Our study provides new insights into how bacteria use a strategy of remodeling the ER dynamics
414 for its benefit. Domingues et al.,2014 and Chen et al.,2021 have highlighted the importance of
415 steA for the active division of SCV [48,71]. Our data supports their findings and suggests the possible
416 role of steA in recruiting the ER and facilitating SCV fission. Interestingly, where wild-type STM
417 can easily divide along with SCV, while loss of function of steA hampers 30% SCV division with
418 marked less colocalization with ER, suggesting there can be several other effector proteins that
419 might facilitate the contacts between ER and SCV. As reported by Chen et al.,2021 about the
420 coordinated role of steA, sopD2, and sifA in successful SCV division, our data explains the newly
421 identified role of steA in the process. Since these effectors have coordinated roles, it will be
422 interesting to understand how individual bacterial effectors are crucial in the complete fission of
423 SCV. Several host proteins have also been linked with SCV division as the absence of those host
424 proteins such as PLEKHM1 and ESCRT-3 leads to SCV carrying multiple bacteria [59,72]. Within the
425 cell, SCV acts as an autonomous organelle that has acquired a vacuolar membrane from the host
426 system which also synchronously divides along with bacterial division. The machinery regulating
427 the SCV division could be difficult to identify because these fission events are very transient in
428 nature. As per literature evidence, both host system and bacterial effectors could be equally
429 involved in this process to execute successful fission. The complete knowledge of fission
430 machinery can be used as a targeted approach to inhibit bacterial proliferation during infection.

Declaration of interest:

The authors declare no competing interests.

Acknowledgement:

This work was funded by the DAE SRC fellowship (DAE00195),DST (FIST), and UGC is sincerely acknowledged. DC acknowledges the ASTRA Chair professorship grant from IISc and TATA innovation fellowship grant. UC sincerely acknowledges IISc GATE fellowship for financial support.

References:

1. Haraga, A., Ohlson, M.B., and Miller, S.I. (2008). Salmonellae interplay with host cells. *6*, 53–66. 10.1038/nrmicro1788.

2. Brenner, F.W., Villar, R.G., Angulo, F.J., Tauxe, R., and Swaminathan, B. (2000). GUEST COMMENTARY Salmonella Nomenclature.

3. Pradhan, D., and Devi Negi, V. (2019). Stress-induced adaptations in Salmonella: A ground for shaping its pathogenesis. Preprint at Elsevier GmbH, 10.1016/j.micres.2019.126311 10.1016/j.micres.2019.126311.

4. Criss, A.K., and Casanova, J.E. (2003). Coordinate regulation of Salmonella enterica serovar typhimurium invasion of epithelial cells by the Arp2/3 complex and Rho GTPases. Infect Immun *71*, 2885–2891. 10.1128/IAI.71.5.2885-2891.2003.

5. Zhou, D., Chen, L.M., Hernandez, L., Shears, S.B., and Galán, J.E. (2001). A Salmonella inositol polyphosphatase acts in conjunction with other bacterial effectors to promote host cell actin cytoskeleton rearrangements and bacterial internalization. Mol Microbiol *39*, 248–260. 10.1046/j.1365-2958.2001.02230.x.

6. Bakshi, C.S., Singh, V.P., Wood, M.W., Jones, P.W., Wallis, T.S., and Galyov, E.E. (2000). Identification of SopE2, a Salmonella Secreted Protein Which Is Highly Homologous to SopE and Involved in Bacterial Invasion of Epithelial Cells.

7. Hardt, W.-D., Chen, L.-M., Schuebel, K.E., Bustelo, X.R., and Galá, J.E. (1998). S. typhimurium Encodes an Activator of Rho GTPases that Induces Membrane Ruffling and Nuclear Responses in Host Cells.

8. Boddy, K.C., Zhu, H., D'Costa, V.M., Xu, C., Beyrakhova, K., Cygler, M., Grinstein, S., Coyaud, E., Laurent, E.M.N., St-Germain, J., et al. (2021). Salmonella effector SopD promotes plasma membrane scission by inhibiting Rab10. Nat Commun *12*. 10.1038/s41467-021-24983-z.

9. Gorvel, J.-P., and Méresse, S. (2001). Maturation steps of the Salmonella-containing vacuole.

10. Drecktrah, D., Levine-Wilkinson, S., Dam, T., Winfree, S., Knodler, L.A., Schroer, T.A., and Steele-Mortimer, O. (2008). Dynamic behavior of salmonella-induced

membrane tubules in epithelial cells. Traffic *9*, 2117–2129. 10.1111/j.1600-0854.2008.00830.x.

11. Garcia-del Portillo, Fran., Zwick, M.B., Yin Leung, K., and Brett Finlay, B. (1993). Salmonella induces the formation of filamentous structures containing lysosomal membrane glycoproteins in epithelial cells.

12. Santos, J.C., Duchateau, M., Fredlund, J., Weiner, A., Mallet, A., Schmitt, C., Matondo, M., Hourdel, V., Chamot-Rooke, J., and Enninga, J. (2015). The COPII complex and lysosomal VAMP7 determine intracellular Salmonella localization and growth. Cell Microbiol *17*, 1699–1720. 10.1111/cmi.12475.

13. Reuter, T., Vorwerk, S., Liss, V., Chao, T.C., Hensel, M., and Hansmeier, N. (2020). Proteomic Analysis of Salmonella-modified Membranes Reveals Adaptations to Macrophage Hosts. Molecular and Cellular Proteomics *19*, 900–912. 10.1074/mcp.RA119.001841.

14. Eswarappa, S.M., Negi, V.D., Chakraborty, S., Sagar, B.K.C., and Chakravortty, D. (2010). Division of the Salmonella-containing vacuole and depletion of acidic lysosomes in Salmonella-infected host cells are novel strategies of Salmonella enterica to avoid lysosomes. Infect Immun *78*, 68–79. 10.1128/IAI.00668-09.

15. Buchmeiert, N.A., and Heffront, F. (1991). Inhibition of Macrophage Phagosome-Lysosome Fusion by Salmonella typhimurium.

16. Salmonella maintains the integrity of its intracellular vacuole through the action of SifA.pdf.

17. Holden, D.W. (2002). Trafficking of the Salmonella vacuole in macrophages. Preprint, 10.1034/j.1600-0854.2002.030301.x 10.1034/j.1600-0854.2002.030301.x.

18. Friedman J.R., Lackner L.L., West M. DiBenedetto J.R., Nunnari J., and Voeltz G.K. (2011). ER tubules mark site of mitochondrial division. Science 10.1126/science.1207385

19. Fernández-Busnadiego, R., Saheki, Y., and De Camilli, P. (2015). Three-dimensional architecture of extended synaptotagmin-mediated endoplasmic reticulum-plasma membrane contact sites. Proc Natl Acad Sci U S A *112*, E2004–E2013. 10.1073/pnas.1503191112.

20. Wong, Y.C., Ysselstein, D., and Krainc, D. (2018). Mitochondria-lysosome contacts regulate mitochondrial fission via RAB7 GTP hydrolysis. Nature *554*, 382–386. 10.1038/nature25486.

503 21. Wang, H.-J., Guay, G., Pogan, L., Sauvé, R., and Nabi, I.R. (2000). JCB Report
504 Calcium Regulates the Association between Mitochondria and a Smooth
505 Subdomain of the Endoplasmic Reticulum.

506 22. Rowland, A.A., Chitwood, P.J., Phillips, M.J., and Voeltz, G.K. (2014). ER contact
507 sites define the position and timing of endosome fission. Cell *159*, 1027–1041.
508 10.1016/j.cell.2014.10.023.

509 23. Ji, W.K., Chakrabarti, R., Fan, X., Schoenfeld, L., Strack, S., and Higgs, H.N.
510 (2017). Receptor-mediated Drp1 oligomerization on endoplasmic reticulum.
511 Receptor-mediated Drp1 oligomerization on endoplasmic reticulum *216*, 190538.
512 10.1101/190538.

513 24. Smirnova, E., Griparic, L., Shurland, D., and Bliek, A.M. Van Der (2001).
514 Dynamin-related Protein Drp1 Is Required for Mitochondrial Division in
515 Mammalian Cells. *12*, 2245–2256.

516 25. Stanhope, R., Flora, E., Bayne, C., and Derré, I. (2017). IncV, a FFAT motif-
517 containing Chlamydia protein, tethers the endoplasmic reticulum to the pathogen-
518 containing vacuole. Proc Natl Acad Sci U S A *114*, 12039–12044.
519 10.1073/pnas.1709060114.

520 26. Boncompain, G., Müller, C., Meas-Yedid, V., Schmitt-Kopplin, P., Lazarow, P.B.,
521 and Subtil, A. (2014). The intracellular bacteria Chlamydia hijack peroxisomes and
522 utilize their enzymatic capacity to produce bacteria-specific phospholipids. PLoS
523 One *9*. 10.1371/journal.pone.0086196.

524 27. Sedzicki, J., Tschon, T., Low, S.H., Willemart, K., Goldie, K.N., Letesson, J.J.,
525 Stahlberg, H., and Dehio, C. (2018). 3D correlative electron microscopy reveals
526 continuity of Brucellacontaining vacuoles with the endoplasmic reticulum. J Cell
527 Sci *131*. 10.1242/jcs.210799.

528 28. Li, M., Tripathi-Giesgen, I., Schulman, B.A., Baumeister, W., and Wilfling, F.
529 (2023). In situ snapshots along a mammalian selective autophagy pathway. Proc
530 Natl Acad Sci U S A *120*. 10.1073/pnas.2221712120.

531 29. Datsenko, K.A., and Wanner, B.L. (2000). One-step inactivation of chromosomal
532 genes in Escherichia coli K-12 using PCR products.

533 30. Wang, S., Tukachinsky, H., Romano, F.B., and Rapoport, T.A. (2016). Cooperation
534 of the ER-shaping proteins atlastin, lunapark, and reticulons to generate a tubular
535 membrane network. 10.7554/eLife.18605.001.

536 31. Shibata, Y., Voss, C., Rist, J.M., Hu, J., Rapoport, T.A., Prinz, W.A., and Voeltz,
537 G.K. (2008). The reticulon and Dp1/Yop1p proteins form immobile oligomers in
538 the tubular endoplasmic reticulum. Journal of Biological Chemistry *283*, 18892–
539 18904. 10.1074/jbc.M800986200.

540 32. Zurek, N., Sparks, L., and Voeltz, G. (2011). Reticulon short hairpin transmembrane
541 domains are used to shape ER tubules. Traffic *12*, 28–41. 10.1111/j.1600-
542 0854.2010.01134.x.

543 33. Singh, V., Erady, C., and Balasubramanian, N. (2018). Cell-matrix adhesion
544 controls Golgi organization and function through Arf1 activation in anchorage-
545 dependent cells. J Cell Sci *131*. 10.1242/jcs.215855.

546 34. Marwaha, R., Arya, S.B., Jagga, D., Kaur, H., Tuli, A., and Sharma, M. (2017). The
547 Rab7 effector PLE KHM1 binds Arl8b to promote cargo traffic to lysosomes.
548 Journal of Cell Biology *216*, 1051–1070. 10.1083/jcb.201607085.

549 35. Alshareef, M.H., Hartland, E.L., and McCaffrey, K. (2021). Effectors targeting the
550 unfolded protein response during intracellular bacterial infection. Preprint at MDPI
551 AG, 10.3390/microorganisms9040705 10.3390/microorganisms9040705.

552 36. Cirone, M. (2021). Er stress, upr activation and the inflammatory response to viral
553 infection. Viruses *13*. 10.3390/v13050798.

554 37. Yamamoto, K., Sato, T., Matsui, T., Sato, M., Okada, T., Yoshida, H., Harada, A.,
555 and Mori, K. (2007). Transcriptional Induction of Mammalian ER Quality Control
556 Proteins Is Mediated by Single or Combined Action of ATF6α and XBP1. Dev Cell
557 *13*, 365–376. 10.1016/j.devcel.2007.07.018.

558 38. Yoshida, H., Okada, T., Haze, K., Yanagi, H., Yura, T., Negishi, M., and Mori, K.
559 (2000). ATF6 Activated by Proteolysis Binds in the Presence of NF-Y (CBF)
560 Directly to the cis-Acting Element Responsible for the Mammalian Unfolded
561 Protein Response.

562 39. Li, M., Tripathi-Giesgen, I., Schulman, B.A., Baumeister, W., and Wilfling, F.
563 (2023). In situ snapshots along a mammalian selective autophagy pathway. Proc
564 Natl Acad Sci U S A *120*. 10.1073/pnas.2221712120.

565 40. Sriburi, R., Jackowski, S., Mori, K., and Brewer, J.W. (2004). XBP1: A link
566 between the unfolded protein response, lipid biosynthesis, and biogenesis of the
567 endoplasmic reticulum. Journal of Cell Biology *167*, 35–41.
568 10.1083/jcb.200406136.

41. Wu, H., Carvalho, P., and Voeltz, G.K. (2018). Here, there, and everywhere: The importance of ER membrane contact sites. Science (1979) *361*. 10.1126/science.aan5835.

42. Lee, J.E., Cathey, P.I., Wu, H., Parker, R., and Voeltz, G.K. (2020). Endoplasmic reticulum contact sites regulate the dynamics of membraneless organelles. Science (1979) *367*. 10.1126/science.aay7108.

43. Voeltz, G.K., Prinz, W.A., Shibata, Y., Rist, J.M., and Rapoport, T.A. (2006). A Class of Membrane Proteins Shaping the Tubular Endoplasmic Reticulum. Cell *124*, 573–586. 10.1016/J.CELL.2005.11.047.

44. Buchmeiert, N.A., and Heffront, F. (1991). Inhibition of Macrophage Phagosome-Lysosome Fusion by Salmonella typhimurium.

45. Hoyer, M.J., Chitwood, P.J., Ebmeier, C.C., Striepen, J.F., Qi, R.Z., Old, W.M., and Voeltz, G.K. (2018). A Novel Class of ER Membrane Proteins Regulates ER-Associated Endosome Fission. Cell *175*, 254-265.e14. 10.1016/j.cell.2018.08.030.

46. Smirnova, E., Griparic, L., Shurland, D.-L., and Van Der Bliek, A.M. (2001). Dynamin-related Protein Drp1 Is Required for Mitochondrial Division in Mammalian Cells.

47. Ji, W.K., Hatch, A.L., Merrill, R.A., Strack, S., and Higgs, H.N. (2015). Actin filaments target the oligomeric maturation of the dynamin GTPase Drp1 to mitochondrial fission sites. Elife *4*, 1–25. 10.7554/eLife.11553.

48. Domingues, L., Holden, D.W., and Mota, L.J. (2014). The Salmonella effector SteA contributes to the control of membrane dynamics of Salmonella-containing vacuoles. Infect Immun *82*, 2923–2934. 10.1128/IAI.01385-13.

49. Case, E.D.R., Smith, J.A., Ficht, T.A., Samuel, J.E., and De Figueiredo, P. (2016). Space: A Final Frontier for Vacuolar Pathogens. Preprint at Blackwell Munksgaard, 10.1111/tra.12382 10.1111/tra.12382.

50. Birmingham, C.L., Smith, A.C., Bakowski, M.A., Yoshimori, T., and Brumell, J.H. (2006). Autophagy controls Salmonella infection in response to damage to the Salmonella-containing vacuole. Journal of Biological Chemistry *281*, 11374–11383. 10.1074/jbc.M509157200.

51. Tilney L.G., Harb O.S., Connelly P.S., Robinson C.G., and Roy C.R.(2001).How the parasitic bacterium Legionella pneumophila modifies its phagosome and transforms it into rough ER implications for conversion of plasma membrane to the ER membrane. Journal of cell science 114, 4637-4650 (2001)

603 52. Kimmey, J.M., and Stallings, C.L. (2016). Bacterial Pathogens versus Autophagy:
604 Implications for Therapeutic Interventions. Preprint at Elsevier Ltd,
605 10.1016/j.molmed.2016.10.008 10.1016/j.molmed.2016.10.008.

606 53. Pujol, C., Klein, K.A., Romanov, G.A., Palmer, L.E., Cirota, C., Zhao, Z., and
607 Bliska, J.B. (2009). Yersinia pestis can reside in autophagosomes and avoid
608 xenophagy in murine macrophages by preventing vacuole acidification. Infect
609 Immun *77*, 2251–2261. 10.1128/IAI.00068-09.

610 54. Rzomp, K.A., Scholtes, L.D., Briggs, B.J., Whittaker, G.R., and Scidmore, M.A.
611 (2003). Rab GTPases are recruited to chlamydial inclusions in both a species-
612 dependent and species-independent manner. Infect Immun *71*, 5855–5870.
613 10.1128/IAI.71.10.5855-5870.2003.

614 55. Mesquita, F.S., Thomas, M., Sachse, M., Santos, A.J.M., Figueira, R., and Holden,
615 D.W. (2012). The Salmonella deubiquitinase Ssel inhibits selective autophagy of
616 cytosolic aggregates. PLoS Pathog *8*. 10.1371/journal.ppat.1002743.

617 56. Zhou, L., Li, Y., Gao, S., Yuan, H., Zuo, L., Wu, C., Huang, R., and Wu, S. (2021).
618 Salmonella spvC Gene Inhibits Autophagy of Host Cells and Suppresses NLRP3 as
619 Well as NLRC4. Front Immunol *12*. 10.3389/fimmu.2021.639019.

620 57. Bastidas, R.J., Elwell, C.A., Engel, J.N., and Valdivia, R.H. (2013). Chlamydial
621 intracellular survival strategies. Cold Spring Harb Perspect Med *3*.
622 10.1101/cshperspect.a010256.

623 58. McGourty, K., Thurston, T.L., Matthews, S.A., Pinaud, L., Mota, L.J., and Holden,
624 D.W. (2012). Salmonella inhibits retrograde trafficking of mannose-6-phosphate
625 receptors and lysosome function. Science (1979) *338*, 963–967.
626 10.1126/science.1227037.

627 59. McEwan, D.G., Richter, B., Claudi, B., Wigge, C., Wild, P., Farhan, H., McGourty,
628 K., Coxon, F.P., Franz-Wachtel, M., Perdu, B., et al. (2015). PLEKHM1 regulates
629 salmonella-containing vacuole biogenesis and infection. Cell Host Microbe *17*, 58–
630 71. 10.1016/j.chom.2014.11.011.

631 60. Sindhwani, A., Arya, S.B., Kaur, H., Jagga, D., Tuli, A., and Sharma, M. (2017).
632 Salmonella exploits the host endolysosomal tethering factor HOPS complex to
633 promote its intravacuolar replication 10.1371/journal.ppat.1006700.

634 61. Bernal-Bayard, J., Cardenal-Muñoz, E., and Ramos-Morales, F. (2010). The
635 salmonella type III secretion effector, Salmonella Leucine-rich Repeat Protein
636 (SlrP), targets the human chaperone ERdj3. Journal of Biological Chemistry *285*,
637 16360–16368. 10.1074/jbc.M110.100669.

638 62. Antoniou, A.N., Lenart, I., Kriston-Vizi, J., Iwawaki, T., Turmaine, M., McHugh,
639 K., Ali, S., Blake, N., Bowness, P., Bajaj-Elliott, M., et al. (2019). Salmonella
640 exploits HLA-B27 and host unfolded protein responses to promote intracellular
641 replication. Ann Rheum Dis *78*, 74–82. 10.1136/annrheumdis-2018-213532.

642 63. Kriston-Vizi, J., Lenart, I., Iwawaki, T., Gould, K., Nesbeth, D., Powis, S.J., and
643 Antoniou, A.N. (2022). Salmonella Exhibit Altered Cellular Localization in the
644 Presence of HLA-B27 and Codistribute with Endo-Reticular Membrane. J Immunol
645 Res *2022*. 10.1155/2022/9493019.

646 64. Lee, J.E., Cathey, P.I., Wu, H., Parker, R., and Voeltz, G.K. (2020). Endoplasmic
647 reticulum contact sites regulate the dynamics of membraneless organelles. Science
648 (1979) *367*. 10.1126/science.aay7108.

649 65. Geddes, K., Worley, M., Niemann, G., and Heffron, F. (2005). Identification of new
650 secreted effectors in Salmonella enterica serovar typhimurium. Infect Immun *73*,
651 6260–6271. 10.1128/IAI.73.10.6260-6271.2005.

652 66. McQuate, S.E., Young, A.M., Silva-Herzog, E., Bunker, E., Hernandez, M., de
653 Chaumont, F., Liu, X., Detweiler, C.S., and Palmer, A.E. (2017). Long-term live-
654 cell imaging reveals new roles for Salmonella effector proteins SseG and SteA. Cell
655 Microbiol *19*. 10.1111/cmi.12641.

656 67. Domingues, L., Ismail, A., Charro, N., Rodríguez-Escudero, I., Holden, D.W.,
657 Molina, M., Cid, V.J., and Mota, L.J. (2016). The Salmonella effector SteA binds
658 phosphatidylinositol 4-phosphate for subcellular targeting within host cells. Cell
659 Microbiol *18*, 949–969. 10.1111/cmi.12558.

660 68. Derré, I., Swiss, R., and Agaisse, H. (2011). The lipid transfer protein CERT
661 interacts with the Chlamydia inclusion protein IncD and participates to ER-
662 Chlamydia inclusion membrane contact sites. PLoS Pathog *7*.
663 10.1371/journal.ppat.1002092.

664 69. Kolodziejek, A.M., Altura, M.A., Fan, J., Petersen, E.M., Cook, M., Brzovic, P.S.,
665 and Miller, S.I. (2019). Salmonella Translocated Effectors Recruit OSBP1 to the
666 Phagosome to Promote Vacuolar Membrane Integrity. Cell Rep *27*, 2147-2156.e5.
667 10.1016/j.celrep.2019.04.021.

668 70. Liu, K., Kong, L., Graham, D.B., Carey, K.L., and Xavier, R.J. (2021). SAC1
669 regulates autophagosomal phosphatidylinositol-4-phosphate for xenophagy-directed
670 bacterial clearance. Cell Rep *36*. 10.1016/j.celrep.2021.109434.

671 71. Chen, D., Burford, W.B., Pham, G., Zhang, L., Alto, L.T., Ertelt, J.M., Winter,
672 M.G., Winter, S.E., Way, S.S., and Alto, N.M. (2021). Systematic reconstruction of

673 an effector-gene network reveals determinants of Salmonella cellular and tissue
674 tropism. Cell Host Microbe *29*, 1531-1544.e9. 10.1016/j.chom.2021.08.012.

675 72. Göser, V., Kehl, A., Röder, J., and Hensel, M. (2020). Role of the ESCRT-III
676 complex in controlling integrity of the Salmonella-containing vacuole. Cell
677 Microbiol *22*. 10.1111/cmi.13176.

678

679

680

681

682

683

684

Graphical Abstract

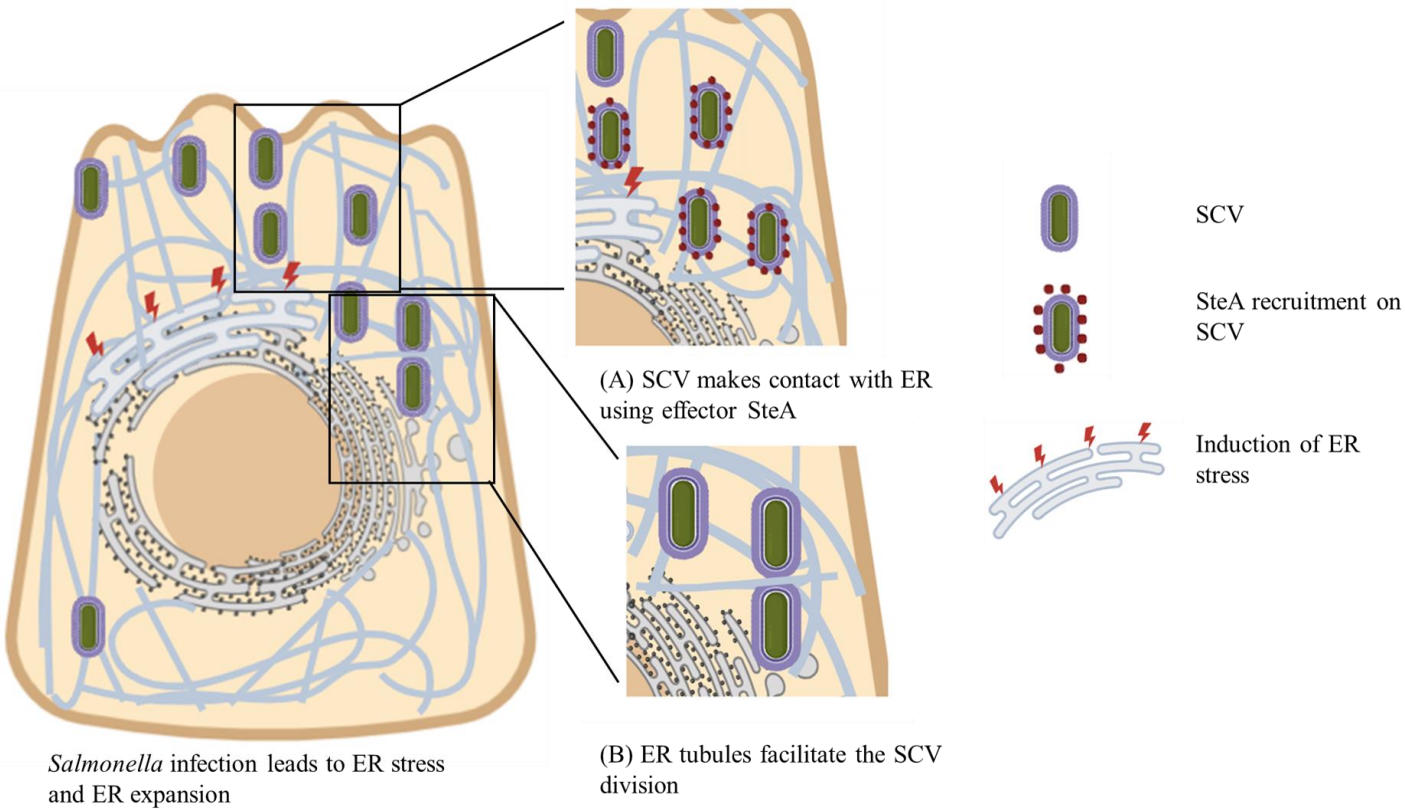

Fig:1 *Salmonella* infection leads to the activation of UPR and expansion of the Endoplasmic Reticulum

1A

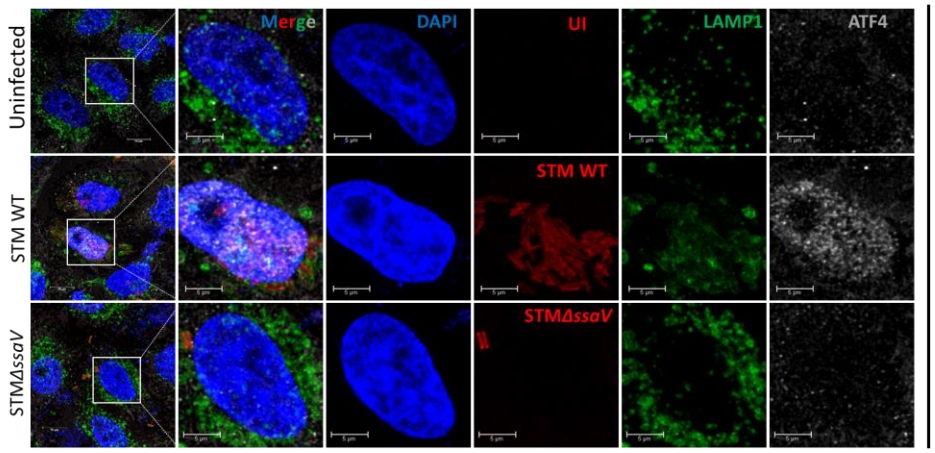

1B

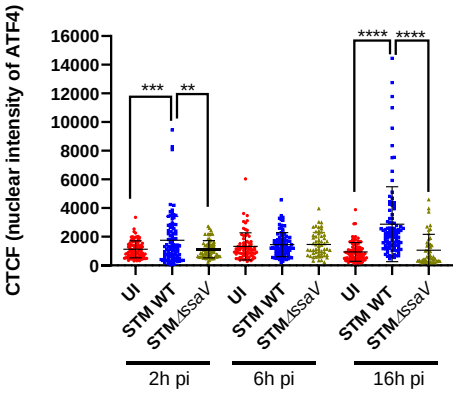

1C

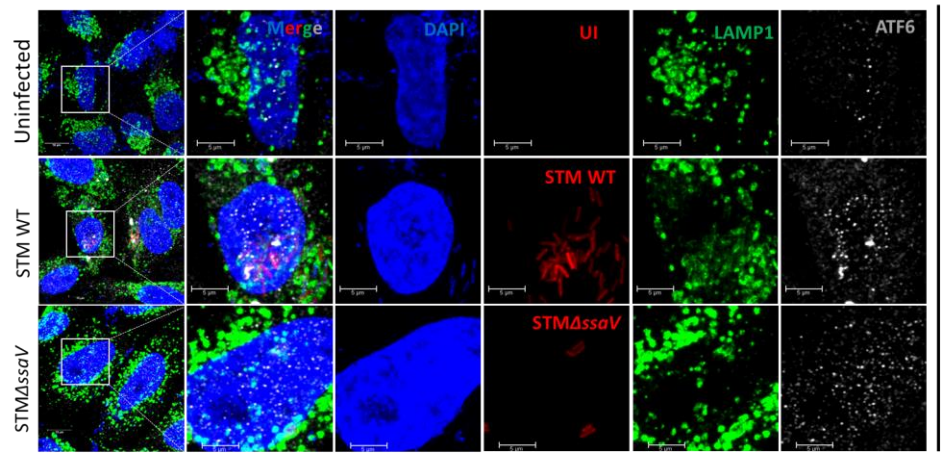

1D

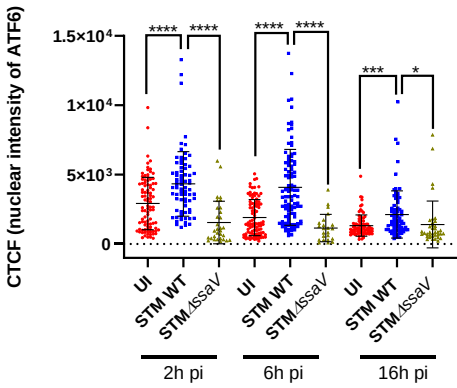

1E

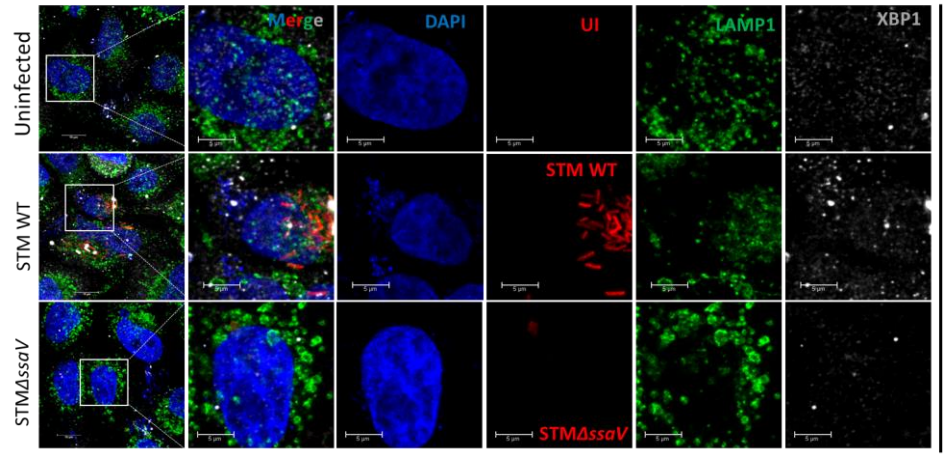

1F

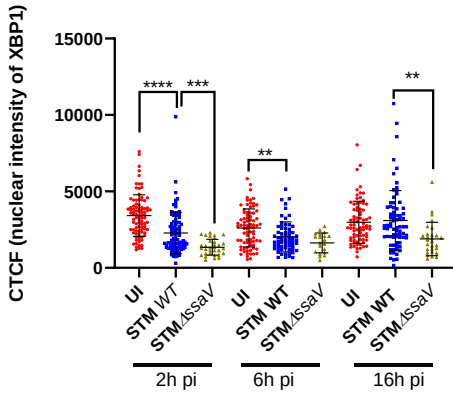

1G

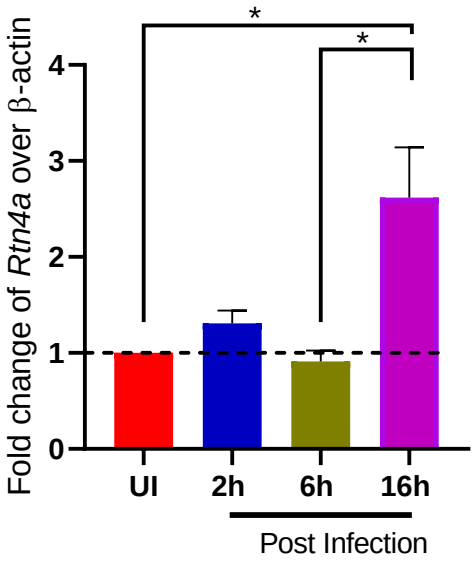
Fold change of *Rtn4a* over β-actin
0
1
2
3
4
*
*
UI
2h
6h
16h
Post Infection

1H

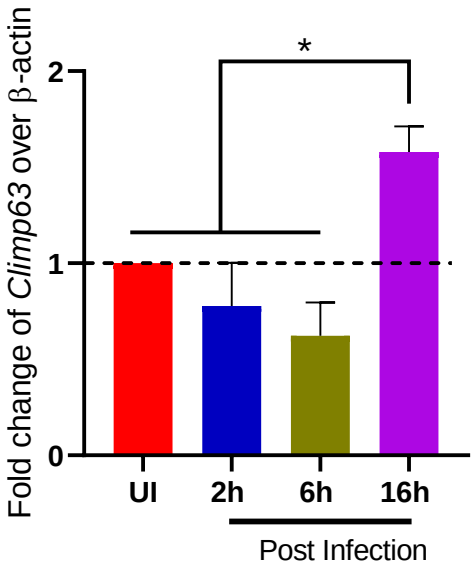
Fold change of *Climp63* over β-actin
0
1
2
*
UI
2h
6h
16h
Post Infection

1I

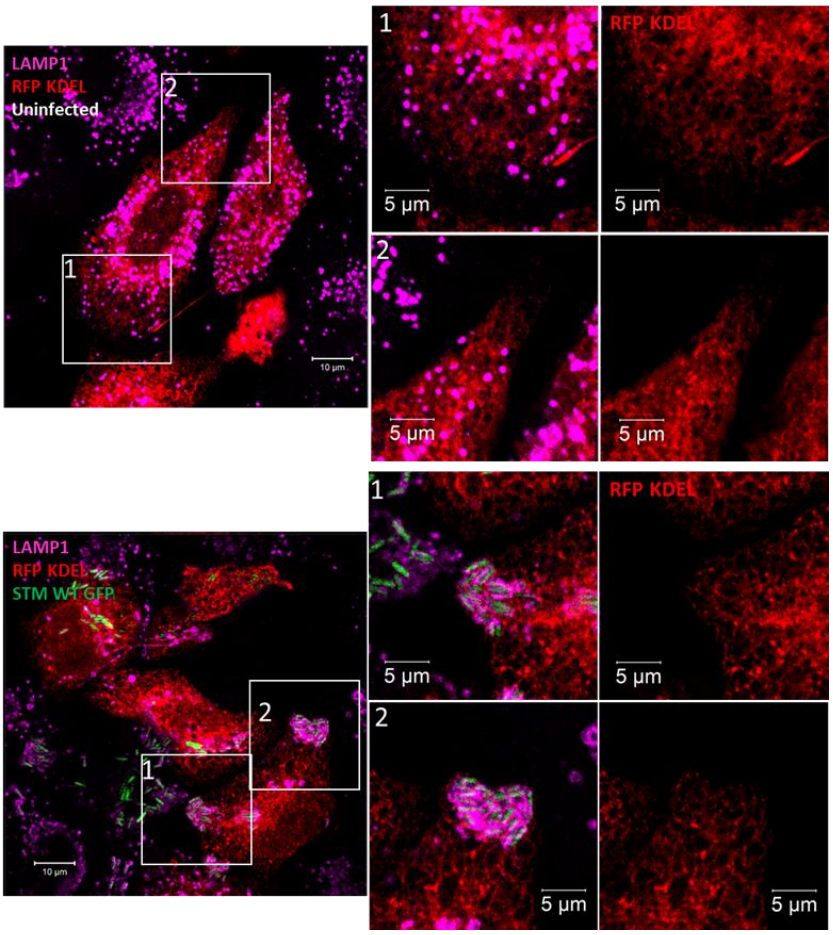
LAMP1
RFP KDEL
Uninfected
1
2
10 µm
RFP KDEL
5 µm
LAMP1
RFP KDEL
STM WT GFP

1J

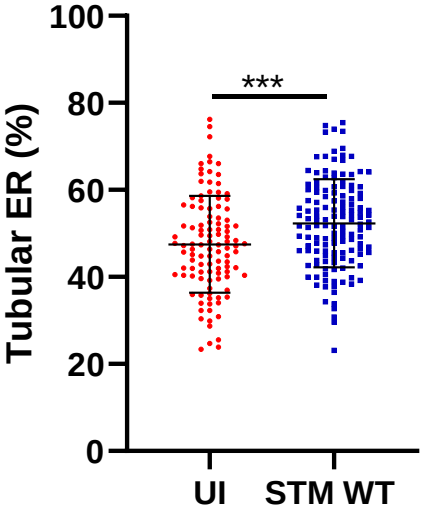
Tubular ER (%)
0
20
40
60
80
100
***
UI
STM WT

Fig:1-*Salmonella* infection leads to the activation of UPR and expansion of the Endoplasmic Reticulum (A) Representative confocal microscopic images of uninfected and infected HeLa cells with STM WT mCh or STM*ΔssaV* mCh at MOI 10, 16h post-infection and immuno-stained against ATF4, LAMP1 and DAPI. (B) Represents the quantification of Cell Total Corrected Fluorescence (CTCF) intensity of ATF4 inside the nucleus, N=4, n=20-30 cell per experiment, data is representative of mean±SD (C) Representative confocal microscopic images of uninfected and infected HeLa cells with STM WT mCh or STM*ΔssaV* mCh at MOI 10, 16h post infection and immuno-stained against ATF6, LAMP1 and DAPI. (D) Represents the quantification of Cell Total Corrected Fluorescence (CTCF) intensity of ATF4 inside the nucleus, N=3, n=20-30 cell per experiment, data is representative of mean±SD (E) Representative confocal microscopic images of uninfected and infected HeLa cells with STM WT mCh or STM*ΔssaV* mCh at MOI 10, 16 hour post infection and immuno-stained against XBP1, LAMP1, and DAPI (F) Represents the quantification of Cell Total Corrected Fluorescence (CTCF) intensity of XBP1 inside the nucleus, N=3, n=20-30 cell per experiment, data representative of mean±SD (G) quantitative real-time PCR of *Rtn4a* (H) and *Climp63*, N=3, n=3, Data is representative of mean±SEM (I) confocal microscopic images of Un-infected and infected HeLa cell showing ER expansion (J) Represents the quantification of tubular ER, N=4,n>50 cells per experiment, data is representative of mean±SD. Student's t test was used to analyse the data ****<0.0001, ***<0.001, **<0.01, *<0.05.

Fig 2: Expansion of ER tubules facilitates SCV proliferation and its division

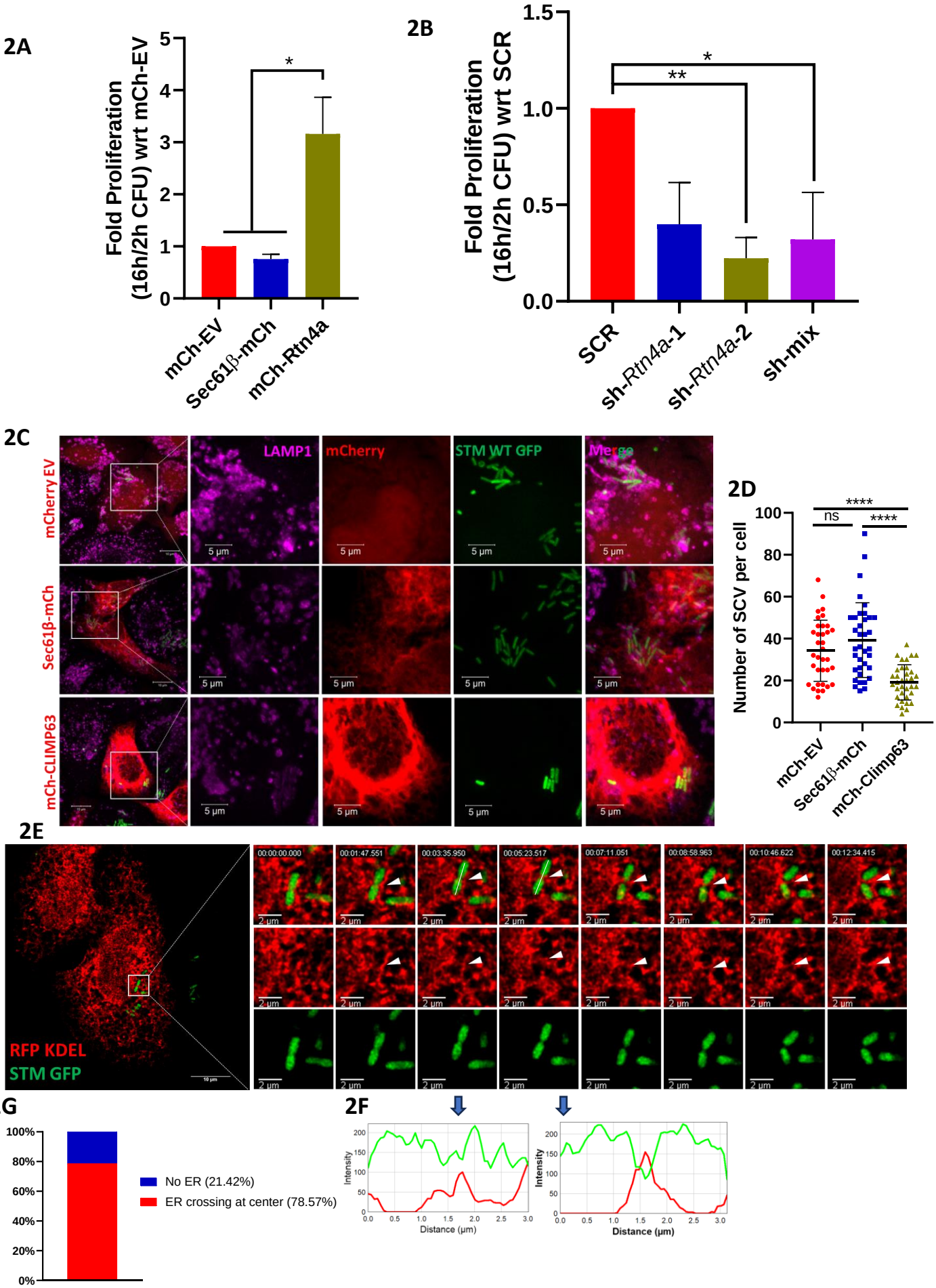

2H

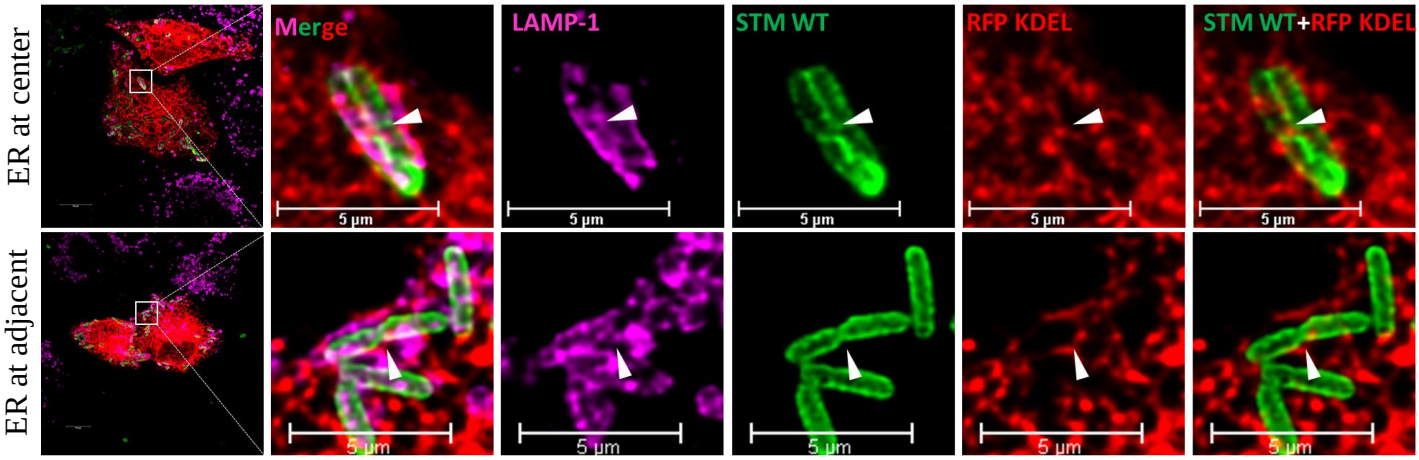

2I

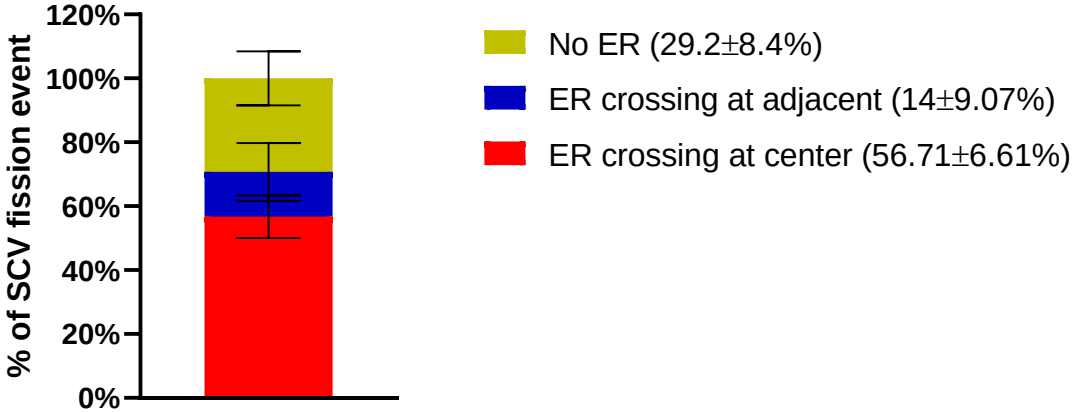

Fig2 Expansion of ER tubules facilitates SCV proliferation and its division (A) Represents the ICSA upon overexpression of Rtn4a, N=3, n=3 mean± SEM(B) ICSA upon Rtn4a knockdown in HeLa cells, N=3, n=3 mean± SEM (C) Representative confocal microscopic images of SCV number per cell upon overexpression of mCh-EV, sec61βs-mCh, and mCh-Climp6 (D) quantification of the number of SCV per cell, representative of N=2, n=20-30 cells per experiment (E) snapshot of live cell imaging of *Salmonella* infected HeLa cells, White arrowhead represent the ER overlap at dividing bacteria. White line along the length of bacteria represent the portion used for line scan. (F) showing the line scan of images. Blue arrows represent the images for which the line scan is analyzed. (G) quantification of SCV fission events marked by ER n=11 fission events from 7 cells (H) Confocal microscopic images representing SCV fission events marked by ER, at center or adjacent (I) quantification of fission events in fixed images marked by ER, n=49 fission events from 31 cells. White arrowhead represent the ER overlap at dividing SCV. Student's t-test was used to analyze the data ****<0.0001, ***<0.001, **<0.01, *<0.05.

Fig 3: *Salmonella* translocated effector steA is crucial for maintaining SCV contacts with ER resulting in a single bacterium per vacuole state

3A

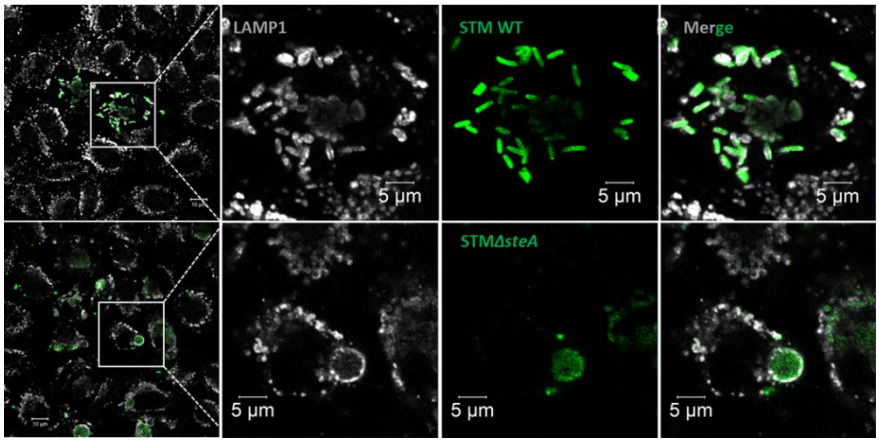

3B

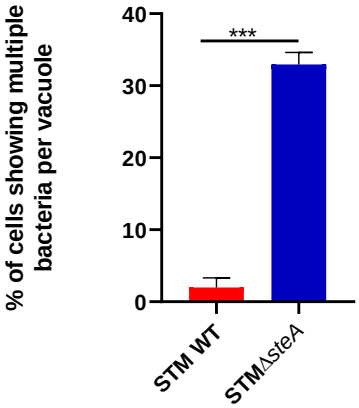

3C

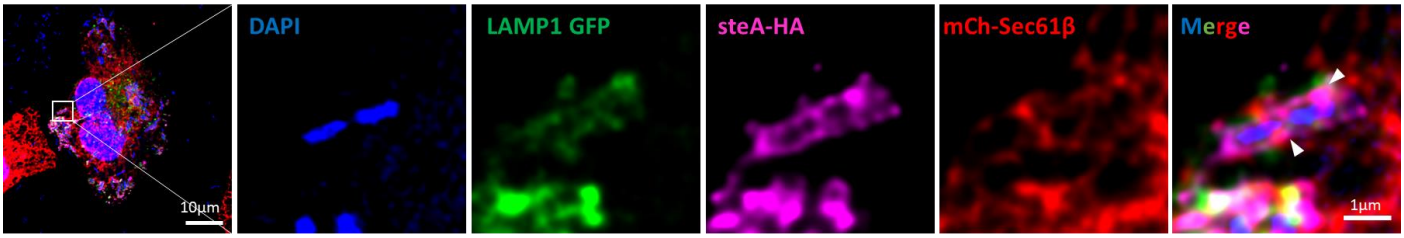

3D

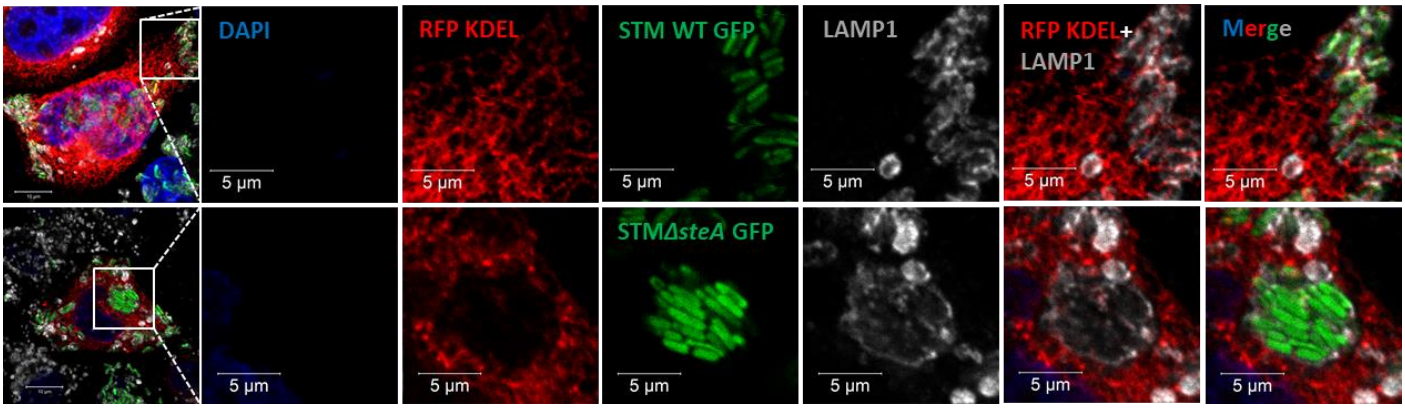

3E

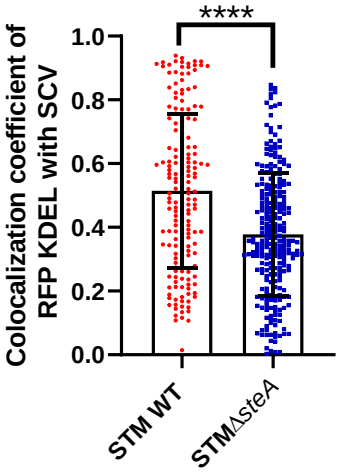

Fig 3: *Salmonella* translocated effector steA is crucial for maintaining SCV contacts with ER resulting in a single bacterium per vacuole state (A) Confocal microscopic images showing SCV formed by STM WT and STM*ΔsteA* (B) Quantification of the number of cells showing multiple bacteria in one vacuole, representative N=3, n>50 cells per experiment, mean±SEM (C) Representative confocal image of infected HeLa cell showing contact between steA-HA and ER, arrowheads represent site of SCV fission and interaction between ER and steA-HA (D) Confocal images represents the colocalization of ER with SCV (E) Quantification of colocalization coefficient of ER marker RFP KDEL with SCV marker LAMP1, Data is representative N=2, n>50 cells per experiment, 16h post infection, mean±SD. Student's t test was used to analyse the data ****<0.0001, ***<0.001, **<0.01, *<0.05.

Fig 4: STM*ΔsteA* shows defect in proliferation inside epithelial cells and pathogenicity in mice in vivo model

4A

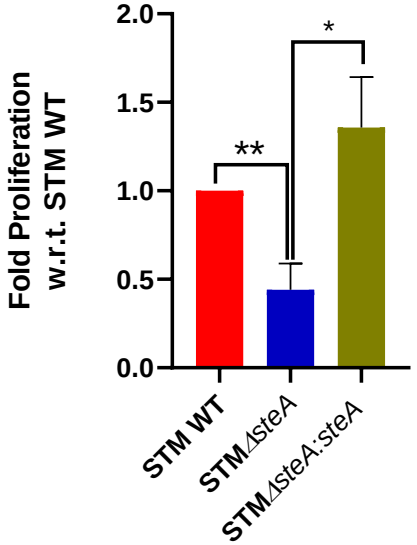

4b

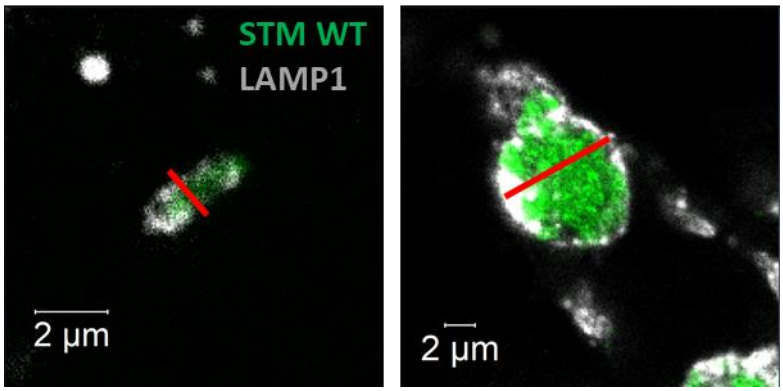

4C

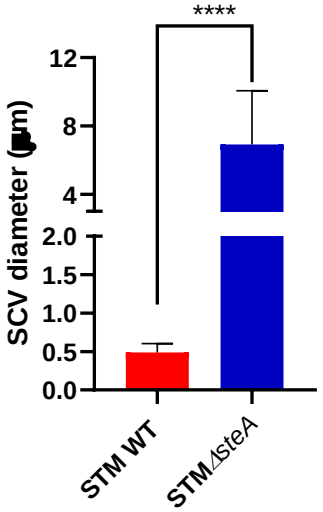

4E

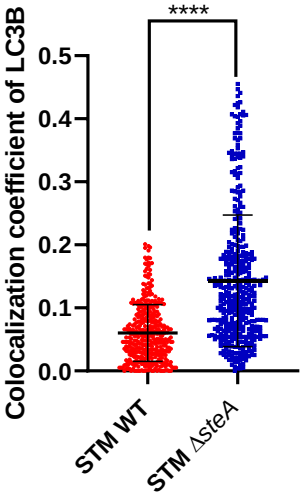

4D

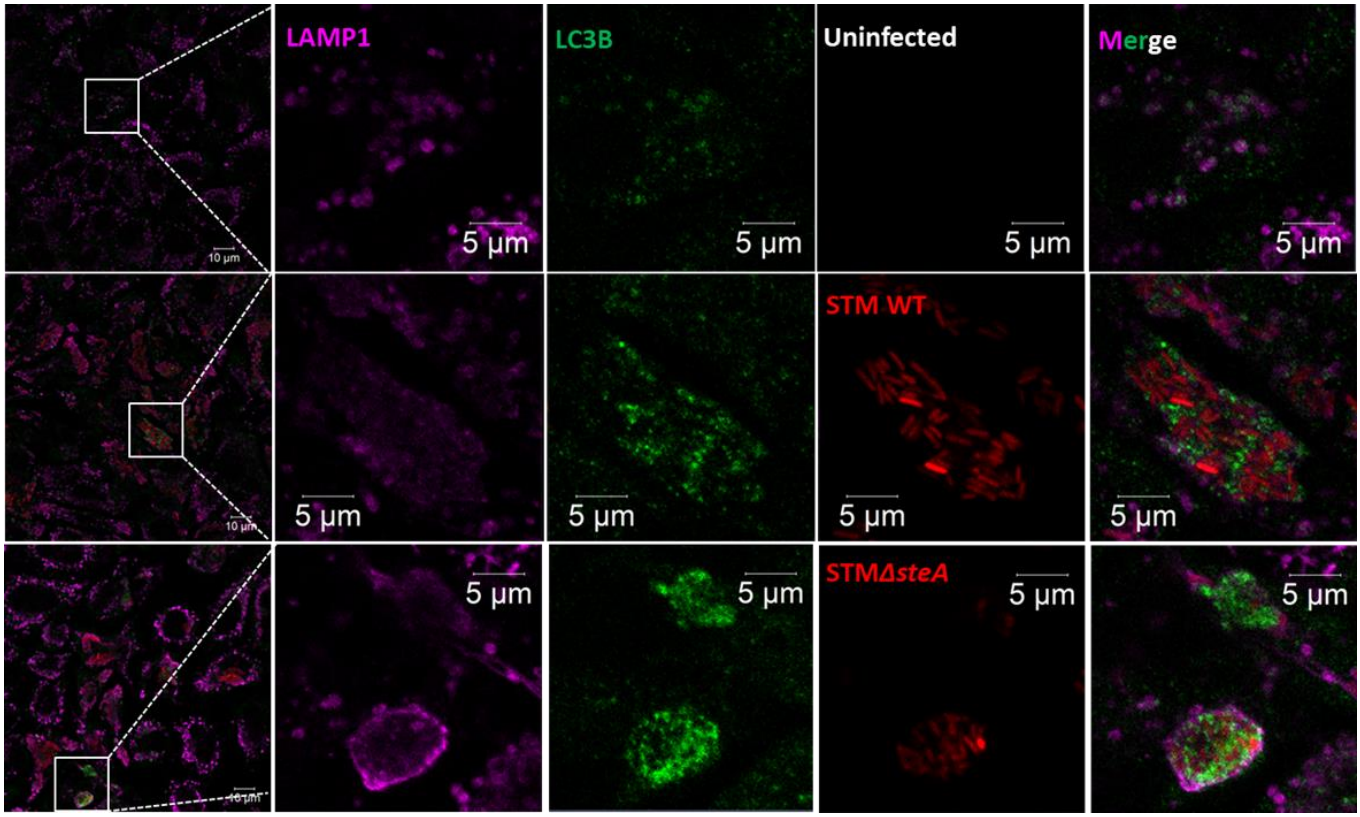

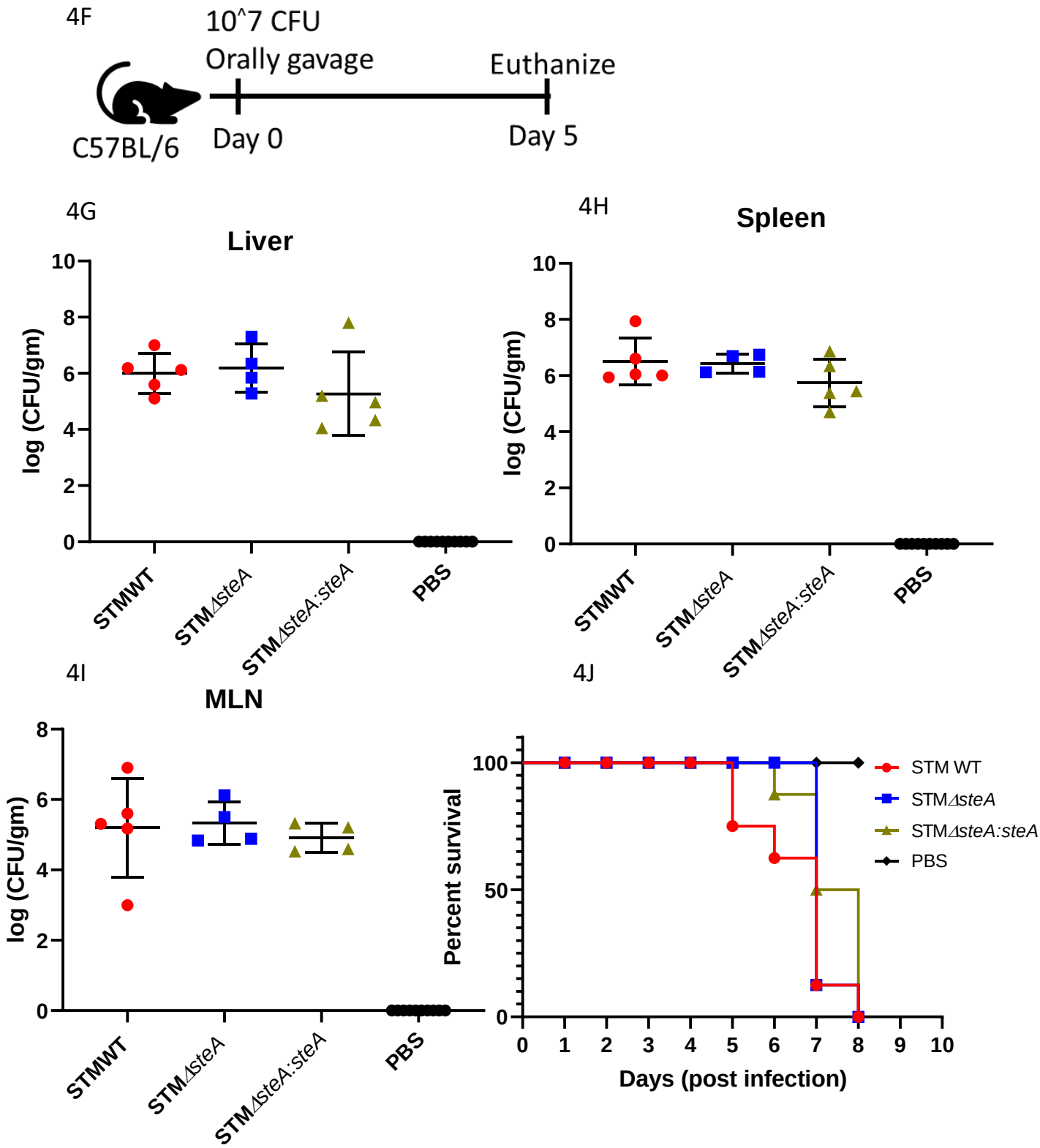

Fig 4: STM*ΔsteA* shows defect in proliferation inside epithelial cells and pathogenicity in mice in vivo model(A) Intracellular survival assay of STM WT, STM*ΔsteA*, and STM*ΔsteA:steA* in HeLa cells, data is representative of N=3,n=3, mean±SEM. (B) Line scan representation to quantify SCV diameter where red line indicates the area used for quantification (C) Quantification of SCV diameter, N=3,n>50 cells per experiment (D) Representative microscopic images showing colocalization of LC3B with SCV (E) Quantification of colocalization coefficient of LC3B with SCV, data is representative of N=3, n>50 cells per experiment, mean±SD (F) outline of experimental procedure of mice infection (G) CFU enumeration in Liver (H) Spleen (I) Mesentric lymph node, data is representative of one experiment, N=2, n=5 animal per cohort (J) survival growth curve of cohort of mice infected with STM WT, STM*ΔsteA*, and STM*ΔsteA:steA*, n=8 mice per cohort. Student's t test was used to analyse the data ****<0.0001, ***<0.001, **<0.01, *<0.05. Mann-Whitney test was performed for animal experiment.

Supplementary Fig:1 *Salmonella* infection leads to the activation of UPR and expansion of the Endoplasmic Reticulum

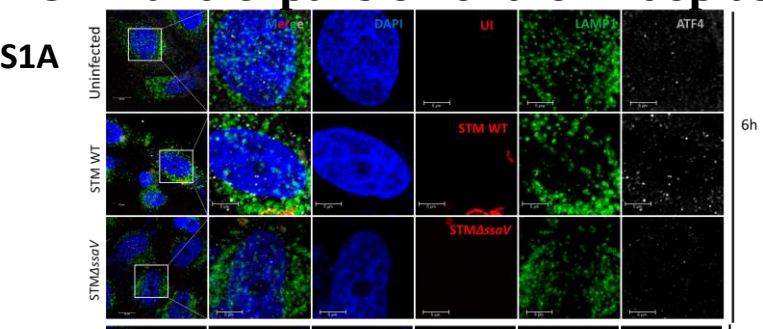

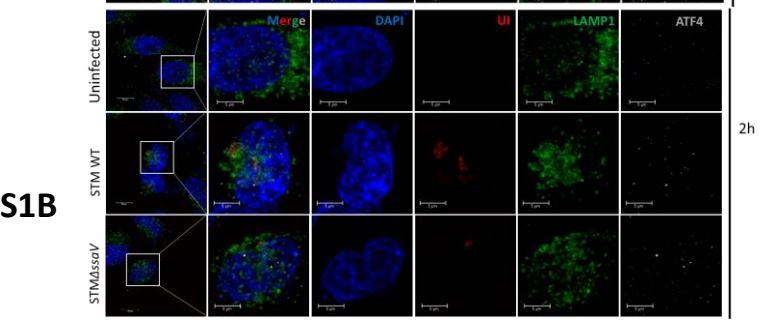

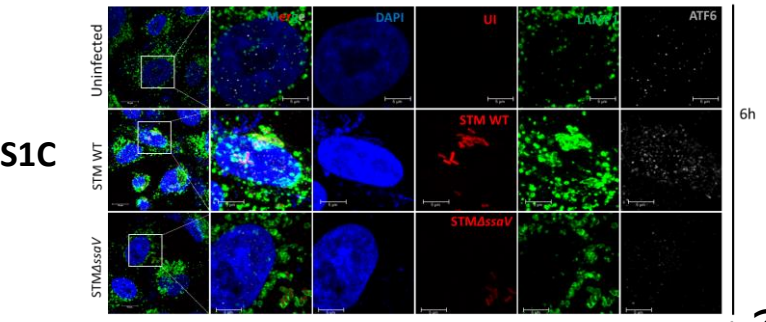

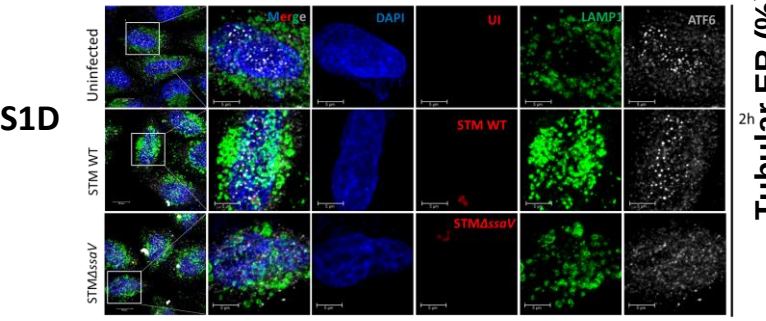

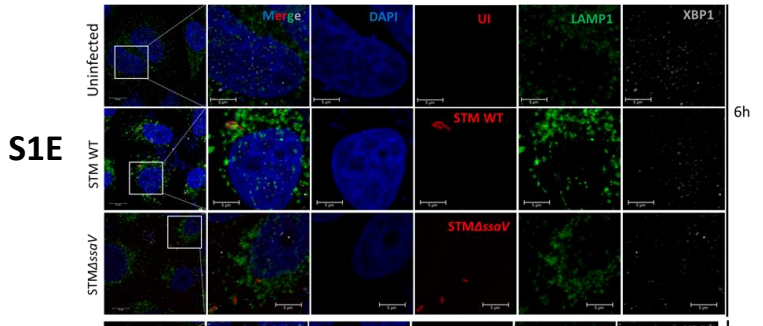

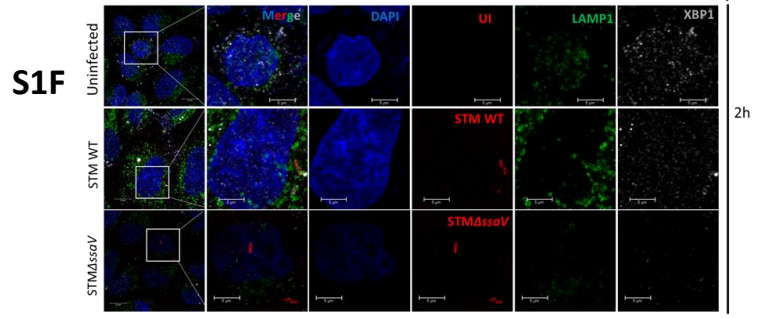

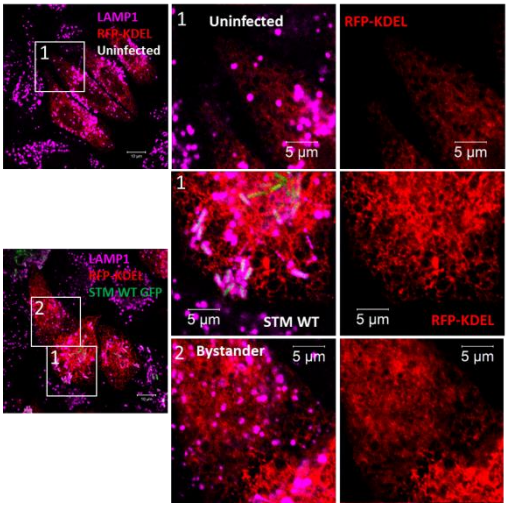

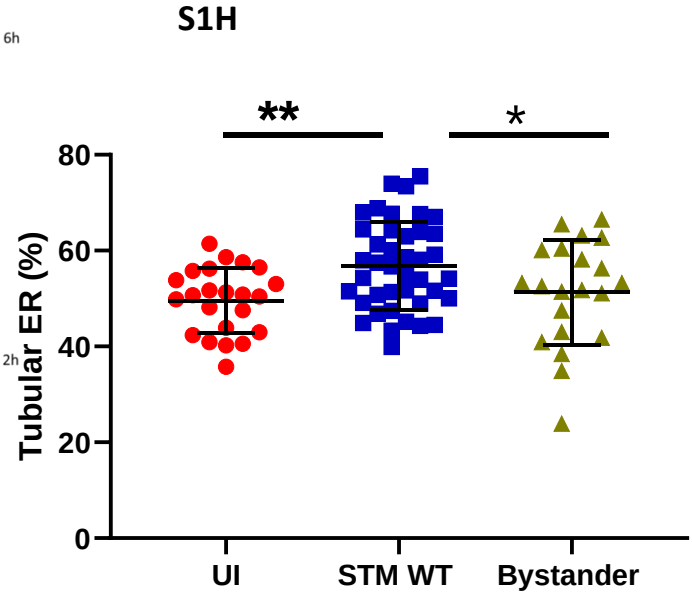

Fig:1 *Salmonella* infection leads to the activation of UPR and expansion of the Endoplasmic Reticulum Representative confocal microscopic images of uninfected, STM WT mCh and STMΔssaV mCh infected cells, immunostained with (S1A) ATF4, LAMP1, DAPI, 6h post infection (S1B) 2h post infection (S1C) ATF6, LAMP1 and DAPI, 6h post infection (S1D) 2h post infection (S1E) XBP1, LAMP1 and DAPI, 6h post infection (S1F) 2h post infection (S1G) Representing uninfected, infected and bystander cell, showing an expansion of ER tubules (S1G) Quantification of ER tubules, N=2, n>20 cells per experiment. . Student's t test was used to analyse the data ****<0.0001, ***<0.001, **<0.01, *<0.05.

Supplementary Fig 2: Expansion of ER tubules facilitates SCV proliferation and its division

S2A

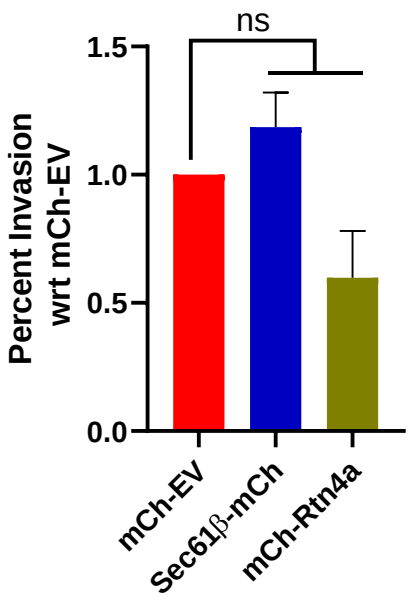

S2B

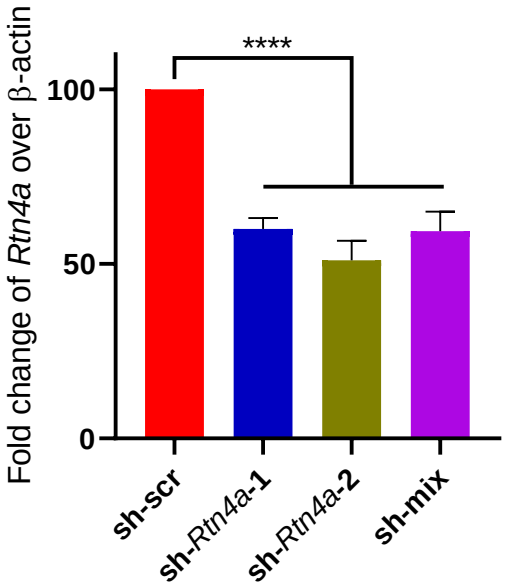

S2C

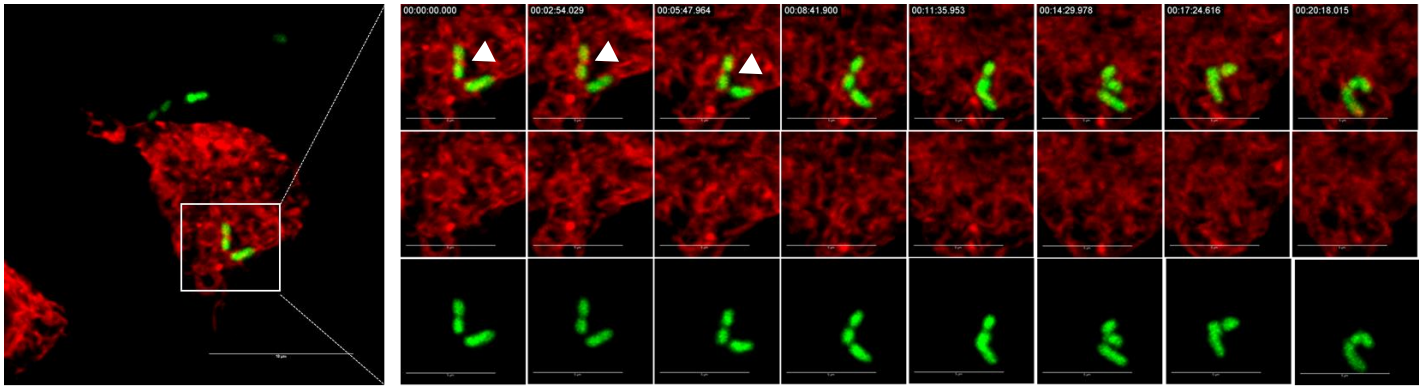

S2D

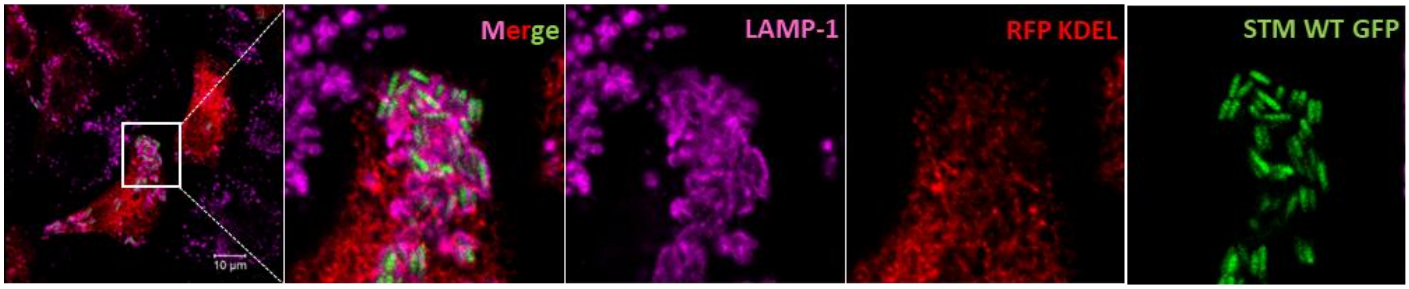

Fig2 Expansion of ER tubules facilitates SCV proliferation and its division (S2A) Percent invasion of STM WT in HeLa cells upon overexpressing mCh-EV, Sec61β-mCh, and Rtn4a-mCh (S2B) Quantitative PCR of *Rtn4a* upon knock down, N=3, n=3, Data is representative of mean±SD (S3C) Live cell imaging snapshots of RAW 264.7 murine macrophage cell line infected with STM WT showing ER overlap at fission site, N=1.(S2D) confocal images of infected HeLa cells showing SCV localization at cell periphery, 16h post infection. Student's t test was used to analyse the data ****<0.0001, ***<0.001, **<0.01, *<0.05.

Supplementry Fig:3 *Salmonella* translocated effector steA is crucial for maintaining SCV contacts with ER resulting in a single bacterium per vacuole state

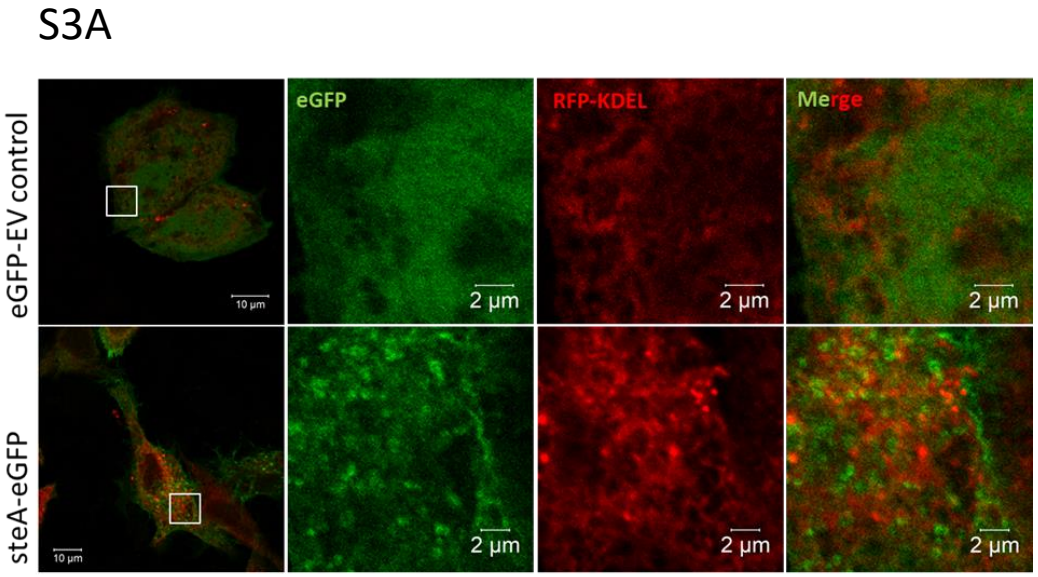

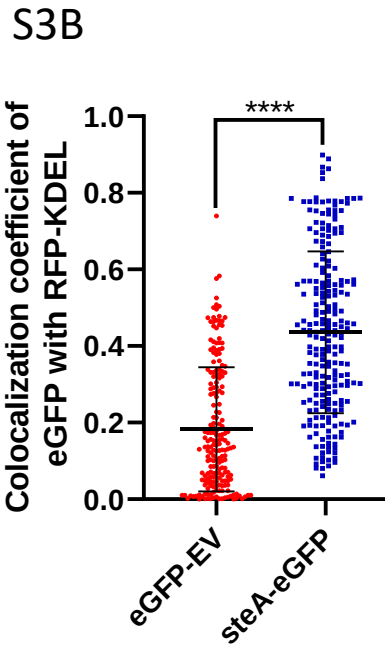

Fig 3: *Salmonella* translocated effector steA is crucial for maintaining SCV contacts with ER resulting in a single bacterium per vacuole state (S3A) Representative microscopic images showing colocalization of eGFP or steA-eGFP with RFP KDEL (ER marker) (S3B) quantification of colocalization coefficient or eGFP with RFP KDEL. Data is representive of N=2, n>50 cells per experiment, mean±SD. Student's t test was used to analyse the data ****<0.0001, ***<0.001, **<0.01, *<0.05.

Supplementary Fig 4: STM*ΔsteA* shows defect in proliferation inside epithelial cells and pathogenicity in mice in vivo model

S4A

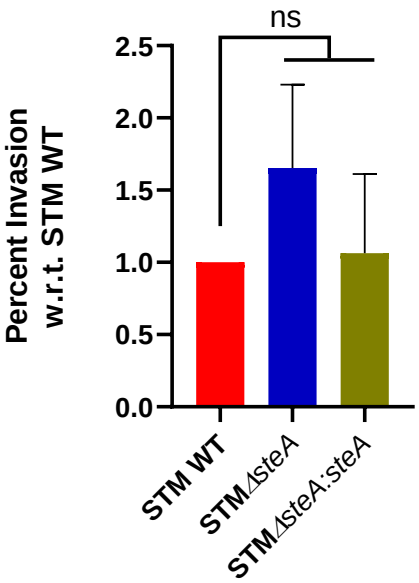

S4C

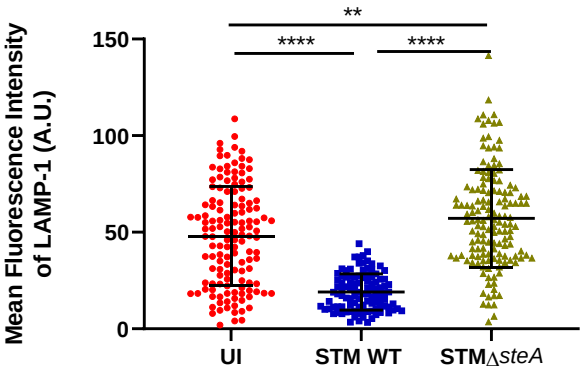

S4B

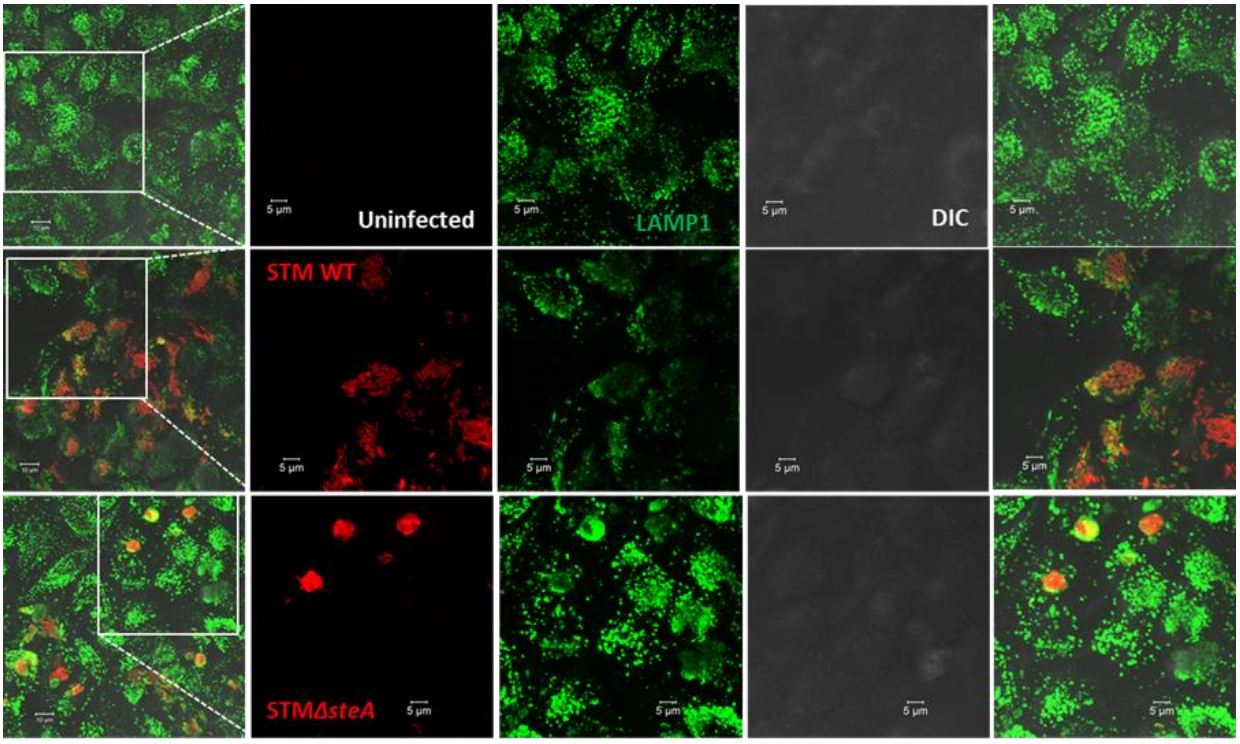

S4D

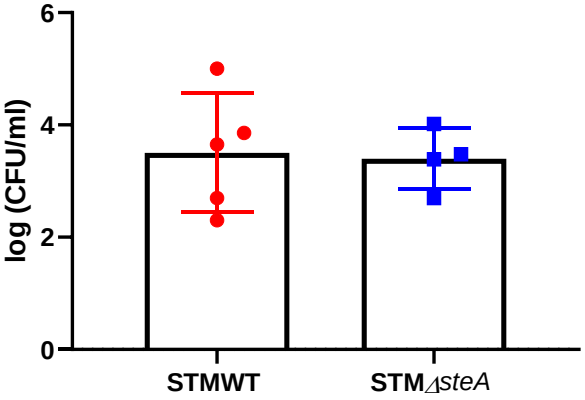

S4E

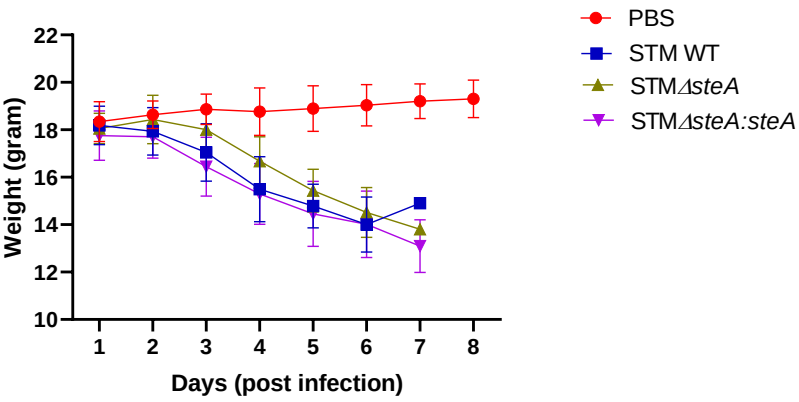

Fig 4: STM*ΔsteA* shows defect in proliferation inside epithelial cells and pathogenicity in mice in vivo model (S4A) percent invasion of STM WT, STMΔsteA, and STMΔsteA:steA in HeLa cells (S4B) Representative images of uninfected and infected HeLa cells with STM WT and STM*ΔsteA* showing intensity of LAMP (S4C) Quantification of mean fluorescence intensity of LAMP1, data is representative of N=3, n>50 cells per experiment, mean±SD (S4D) CFU analysis of STM WT and STMΔsteA in blood sample of C57BL/6 mice, 5th day post oral gavage , N=2, n=5 mice per cohort.(S4E) Represents weight reduction in mice upon infection with STM WT, STM*ΔsteA and* STM*ΔsteA:steA* till 8 days post infection, 8 mice per cohort. Student's t test was used to analyse the data ****<0.0001, ***<0.001, **<0.01, *<0.05.

Supplementary File: Table-1, List of Primers used in this study:

S.No	Primer Name	Sequence (5'-3')
1	steA-KO-FP	CAAATAGTTATGGTAGCGAGCTTTTATGTCGGCCGCCCATCATATGAATATCCTCCTTAG
2	steA-KO-RP	TCAGTTTCTACCTATGCCAGAGCTTTATCAGGAAATAAGCGTGTAGGCTGGAGCTGCTTC
3	steA-eGFP cloning-FP	TTTTTCTCGAGATGCCATATACATCAGTTTCTACC
4	steA-eGFP cloning-RP	TTTTTGGATCCATAATTGTCCAAATAGTTATGG
5	HU-Rtn4a-RT-FP	TCGGGCTCAGTGGATGAGA
6	HU-Rtn4a-RT-RP	GCAGGACAGATGGGAAATCCT
7	HU-Climp63-RT-FP	GCGTCGAGCAGAAGGTGC
8	HU-Climp63-RT-RP	CATGGATCCCATCCGAGAGG
9	Xho1_fwd_Native_promoter_steA_cloning	TTTTTCTCGAGCGGCAGTGATTGCGTTGC
10	HindIII steA-HA_cloning_RP	TTTTTTAAGCTTTTATGCATAATCCGGAACATCATACGGATAATAATTGTCCAAATAGTTATGGTAGCGAGC
11	HU-β-actin-FP	GCCGCCAGCTCACCAT
12	HU-β-actin-RP	TCGTCGCCCACATAGGAATC

Supplementary File: Table:2 List of Antibodies

Antibody	Catalog number
ATF-4	CST-11815s
ATF-6	ATF-6α Antibody (H-280): sc-22799
XBP-1	XBP-1 Antibody (M-186): sc-716
LAMP1	DSHB 1D4B
Anti-Salmonella	Invitrogen- PA1-20811
LC3B	Sigma-L7543

Supplementary File: Table: 3 List of plasmids used for overexpression

Plasmid	Source
1) pHAGE2 mCherry-Rtn4a (Plasmid-86683)	pHAGE2 mCherry-Rtn4a was a gift from Tom Rapoport (Addgene plasmid # 86683)
2) mCh-Climp63 (Plasmid #136293)	mCh-Climp63 was a gift from Gia Voeltz (Addgene plasmid # 136293)
3) RFP-KDEL	RFP KDEL construct was a kind gift from Prof. Nagaraj Balasubramanian
4) LAMP1-GFP	GFP-LAMP1 construct was provided by Prof. Mahak Sharma
5) Sec61β-mCh	mCh sec61β was a kind gift from Prof. Gia Voeltz (Addgene 49155)

List of shRNA plasmids used for knockdown

S.No.	**Target Gene**	**TRC ID**	**Sequence**
1	RTN4 reticulon 4 [*Homo sapiens* (human)]	TRCN0000179649	CCGGGCAGTGTTGATGTGGGTATTTCTCGAGAAATACCCACATCAACACTGCTTTTTTG
2	RTN4 reticulon 4 [*Homo sapiens* (human)]	TRCN0000147624	CCGGGCATATCTGGAATCTGAAGTTCTCGAGAACTTCAGATTCCAGATATGCTTTTTTG